Active Assistive Knee Device

Tina Barsoumian, Jason McGrath, Christina Steele,
Kassidy Utheim, Zachary Zlotnick

August 2019 - May 2020

Major Qualifying Project Report:

Submitted to the Faculty of

Worcester Polytechnic Institute

in partial fulfillment of the requirements for the

Degree of Bachelor of Science in

Mechanical Engineering, Robotics Engineering,

and Biomedical Engineering.

Sponsored by:
Maxon Group

Submitted to:
Professor Selçuk Guçeri
Professor Marko Popovic

Abstract

This project aimed to develop an active assistive knee device to aid the user in their gait cycle and stair ascent and descent. Currently, few devices exist on the market that offer a solution for those desiring a small amount of assistive torque in a low profile, cost-effective design. Experimental and literary research were performed to determine the amount of assistance needed from the device, and the ideal structure. A novel hinge design was created and, once partnered with the electromyograph and motor, provides 10% of the required torque at the knee for the user. Due to COVID-19, the team was unable to fabricate and assemble a working prototype. Improvements include refining the design to be smaller and lighter, and adding a second motor for increased torque.

maxon

Authorship

The team was divided into sub-teams based on their majors of study and skill-sets. The first team was the Mechanical Engineering and Design team, they were responsible for the design of the mechanical hinge system. The second team was the Biomedical and Robotics Engineering team, they worked on the control system for actuating the device.

Mechanical Engineering and Design

The mechanical team consisted of the mechanical engineering majors: Christina Steele, Kassidy Utheim, and Jason McGrath. Kassidy and Christina worked on designing the CAD models of the hinge to incorporate all of the necessary components. They also envisioned the entire system and how it would be attached to the leg. Jason worked on determining the gearing and manufacturing the design. All three members assisted each other in these efforts. The initial decisions of using a hinge system and planetary gears was a group effort.

Biomedical and Robotics Engineering

The control sub-team consisted of the other two members of the team: Tina Barsoumian, a biomedical engineering major and Zachary Zlotnick, a robotics engineering major. Tina worked on the electromyograph (EMG) and getting it to read the user's muscle activation levels. She also focused on the PracticePoint motion capture data acquisition and analysis. Zach worked on acquiring the motor and properly setting it up with the motor controller and battery for use with the device.

Acknowledgements

maxon

Contents

List of Figures

maxon

1   Introduction

This project was created by Professor Selcuk Guçeri, who was diagnosed with polio at a young age. Due to the disease, he has an instability and weakness at his right knee. This affects his walking and stair ascent and descent gait, as he needs to use his upper body to pull himself up using the railings. Professor Guçeri identified this need and potential market, and he believed that creating this technology could benefit himself and others in similar situations. The target market identified for this project are humans with a variety of health-related leg issues which cause an asymmetry between an individual's knee joints and irregular gait patterns. The kinematics and mechanics of motion based on the normal gait cycle and stair ascent and descent were studied. This report's literature review separated assistive knee devices into two forms, active and passive. Passive examples include canes, crutches, or braces. On the other hand, active knee devices are capable of providing energy to their system. Active devices on the market offer full or near-full assistance to the user in the form of an exoskeleton. In order to differentiate the idea from the existing market solutions, the team aimed to create a device that would fit people looking for an exoskeletal design which provides a helping hand in stair motion and walking. The device's lightweight and cost-effective design would ideally allow it to appeal to mainstream users. Additionally, the electromyograph (EMG) provides an intuitive control solution while coupled with a planetary gear system driven by a pancake motor.

The prototype was developed for use on a single leg, however, the device could also be applied to both legs. The team chose to represent the motion of the knee as a simple hinge to provide more freedom over the design and control over the system. The circular hinge houses the gear components that help increase torque assistance. This project aimed to create an active assistive knee device for a gait-impaired human. The device aids the user's knee during daily movements such as walking and ascending and descending stairs. This device is also helpful for those with injuries or post-operations, where a weakness in the knee is present. This design is estimated to provide 10% of a healthy subject's torque at the knee, not offer full replacement.

maxon

By talking to the professors, the team determined that an extra 10% of assistive torque was a feasible goal, given the time and manufacturing constraints. This target is attainable, yet still allows for sufficient assistance of the leg. Target market research defined the primary beneficiary as humans with a variety of health-related leg issues. Through this research, the team determined that a device successfully able to provide this torque at the knee would fill a significant market gap.

2   Background

2.1   Health Problems Associated with the Knee Joint

The knee is the largest joint in the human body and greatly impacts one's mobility and stability. When an individual's knee is deformed, gradually deteriorates, or experiences trauma, a walking aid or knee replacement is commonly prescribed. The Global Total Knee Replacement and Orthopedic Brace Markets are predicted to gross over 5.5 billion dollars by 2024 (Singh, 2019). This market is profitable because 600,000 people are given knee replacements annually, and countless others are rehabilitated with walking aids (Mauney, Connolly, Dr. Aimee V. Hachigian-Gould, Mulcahy, & Chew, 2013). Knee damage originates from a wide variety of causes, but an inadequate knee can share similar symptoms that alert an individual in need of a walking aid or knee replacement. These symptoms include having knee pain while sleeping, a locking feeling in different areas of the knee, hip pain, swelling, and stiffness in the knee. These issues can manifest in the form of losing balance easily, a reduction in mobility due to inability to fully extend the knee, and feet dragging while walking. If untreated, these symptoms have the potential to decrease one's quality of life because they make everyday tasks a burden (Biron Health Group, n.d.). Arthritis plays one of the largest roles in one's ability to retain the strength in their knees and is common in three forms: Osteoarthritis, Rheumatoid Arthritis, and Gout, all resulting in pain and stiffness at the joint. Although the most prominent age range for humans in need of replacements or walking aids ranges from sixty to eighty, younger populations are often still affected by knee deficiencies (NHS, 2019). Musculoskeletal imbalances negatively impact the knee by training knee muscles to be strongest in unnatural positions. Examples include tendinitis, lesions, bursitis (inflamed synovial bursa), and nerve compression (Biron Health Group, n.d.). All imbalances are considered to be a structural deformity or weakness in muscles that support the knee (Campbell & Chittenden, n.d.).

maxon

2.2   Existing Knee Devices

Assistive knee devices can come in two forms, active and passive. Passive devices do not require power to operate; examples include splints, braces, neoprene sleeves, canes, and crutches. Splints keep joints in place and inhibit awkward or harmful motion of the knee. Braces are popular because they work to keep one's bones in place to prevent pain and reduce stress on the tendons. Similarly, neoprene sleeve braces are commonly prescribed, following surgery, to prevent jagged movements that disrupt healing. Canes and crutches reduce pain and strain by transferring one's weight off the knee and onto a support (Orenstein & Sinha, 2018).

Active assistive knee devices differ from passive devices in that they are capable of providing energy to the system. They provide independence to disabled individuals through the ability to conduct tasks that they would otherwise be unable to do. Examples of active knee devices include Cyberdyne's HAL (Single Joint Type), which employs a single motor that provides assistive force to the knee or elbow. This device boast a light, low profile, modular design which is easy to wear and travel with. HAL is controlled by sensors that read muscle signals received by the brain from the nerves. This information is then sent to the motor to perform the desired movement. For normal operation, the device last for 120 minutes (Cyberdyne, 2020).

Ottobock's new C-Brace is a powerful device allowing users with symptoms such as incomplete paraplegia to perform daily tasks. After an individual is fitted with their custom brace, they experience various benefits: natural, controlled gait when walking and descending stairs and a supportive ankle component enabling proper foot motion, and a low profile design that fits under loose clothes. The C-brace is regulated by sensors in the knee joint which track the position, direction, and velocity of the leg 100 times a second. Using this information, the device can determine the amount of support to the leg it should provide via a hydraulic pump (Ottobock, 2018). Due to the premium quality and extra features incorporated in this device, the selling price is $75,000 (Holicky, 2016). Another knee aid exoskeletons, the LegX, exists to provide joint protection for prolonged periods of time by reducing the knee joint and quadriceps muscle forces. The LegX is an

maxon

intelligent system that can identify when the user is walking, ascending and descending stairs, or squatting to provide necessary support for different situations. These devices provide high levels of assistance, but present a large profile on the outside of the user's lower body (SuitX, n.d.).

KEEOGO, developed by B-Temia, is an assistive exoskeleton focused on the lower body of the user. Based on the user's initial movement, the device identifies their intent through multiple sensors. Motors are then used to complete the desired motion by either providing an assistive or resistive force depending on the situation. Additionally, KEEOGO reduces the amount of stress on the user's knee, allowing for increased strength, endurance, and stability (Keeogo, n.d.). The exoskeleton is attached to both knees, and does not secure the feet, pelvis or torso (Mcgibbon et al., 2018). Images of all of these existing devices are shown in figure 1. Reference Appendix 7.3 for more a comparison between existing products in the marketplace.

Figure 1: The existing devices from left to right: Cyberdyne's HAL Single Joint, Ottobock's C-Brace, SuitX's Leg X, B-Temia's KEEOGO. These images are adapted from, (Cyberdyne, n.d.),(Alex Hernandez, 2018),(SuitX, n.d.),(Keeogo, 2015)

2.3 Biomechanics of the Human Knee

2.3.1 Walking

The movements of the human body, focused on in this report, are the walking and stair ascension and descension gait cycles. The walking gait cycle occurs from the point of one foot touching the ground to that same foot touching the ground once again. Based upon observation of the gait cycle, the minimum amount of energy used exists in the

normal gait pattern. During this pattern, there is little to no movement in the head, which can be translated to minimal movement of the torso. This means that nearly all movement of the body during the gait cycle occurs in the legs (Ren, Jones, & Howard, 2007).

The gait cycle consists of two major phases: the stance phase and the swing phase. The stance phase includes the moment the heel strikes the ground, known as heel strike, to the moment the toe leaves the ground, known as toe off. This phase can be split into five subsections as seen in figure 2 below. Likewise, the swing phase consists of the toe off to the heel strike and is split into three subsections (Physiopedia, 2020).
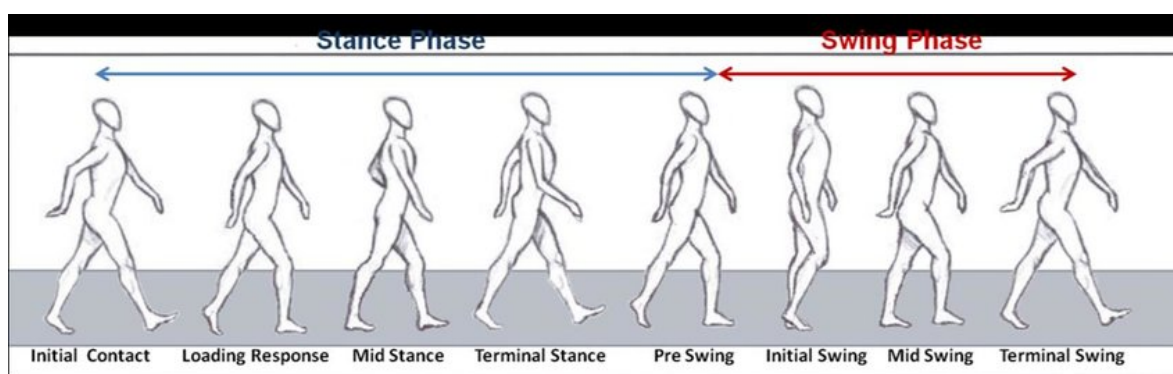
Figure 2: The Walking Gait Cycle, adapted from (Susi, 2015)

During the gait cycle, all joints undergo a great deal of motion. The knee experiences mostly flexion and extension. For the majority of the stance phase, knee flexion remains at an angle less than 20 degrees. However, it does reach an angle of 55 degrees at toe off. The greatest flexion is experienced during the swing phase, reaching a maximum angle of 75 degrees (Morrison, 1970). This flexion can be seen in figure 3 below. The knee also experiences negligible lateral and medial movement. This is why the knee is considered a "screw home" joint (Lafortune, Cavanagh, Sommer, & Kalenak, 1992). A screw home mechanism is the rotation at the knee between the tibia and the femur. This is because the "medial tibial plateau articular surface is longer than lateral tibial plateau" (Karadsheh, 2020). The advantage of a screw home mechanism is that the knee is able to lock, decreasing the work performed by the quadriceps while locked, or while standing ("Screw-home mechanism", 2012).

maxon
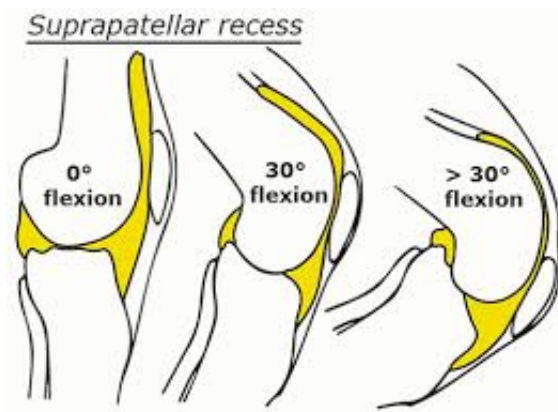
Figure 3: Knee Flexion, adapted from (Van der Plas & Bloem, 2016)

During the stance phase, the knee experiences slight flexion. The motion begins with the initial contact, heel strike, when the knee is in full extension. The knee fully extends due to the contraction of the quadriceps with assistance from the tensor fasciae latae tendon (Morrison, 1970). When the knee is in full extension, all of the cruciate ligaments (ACL, PCL, MCL, LCL) tighten, causing the knee to lock (Neumann et al., 2015). At the end of the heel strike phase, the knee begins to experience flexion. This is caused by the contraction of the hamstrings and the gracilis and sartorius tendons. At the loading response phase, the knee reaches a flexion just under 20 degrees. During midstance, the knee achieve maximum flexion for the stance phase and begins to extend. At terminal stance, when the heel leaves the floor, the knee changes from full extension to initial flexion. The knee continues to flex approximately 50 degrees during the pre-swing phase (Morrison, 1970).
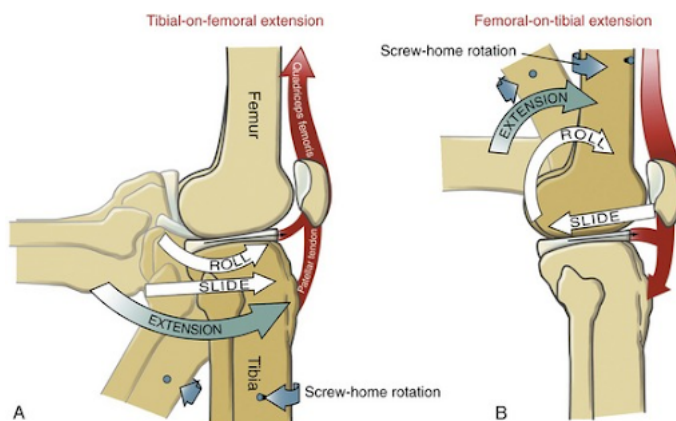
Figure 4: Knee Extension, adapted from (Neumann et al., 2015)

During the swing phase, the knee flexes in order to experience toe off, allowing it to swing forward. In the initial swing, the knee flexes to about 50 degrees and continues until the mid-swing phase, reaching a 60 degree flexion. At the end of the mid swing phase, the knee begins to extend to about 30 degrees, caused by the contraction of the sartorius muscle as well as the quadriceps (Morrison, 1970). Finally, the terminal swing phase occurs when the knee is fully extended and locked. Figure 4 shows the movement of the femur and tibia during extension of the knee (Neumann et al., 2015). For better understanding, a simple depiction of the muscles and tendons by the knee are shown in figure 5.

Figure 5: Tendons in the Leg, adapted from (Elina33, 2014)

Throughout the walking gait cycle, the knee has a maximum joint force of approximately two times a person's body weight. The overall flexion moment while walking is approximately 1.92% of the subjects body weight times meter (BWm) (Kutzner et al., 2010). This is approximately a 0.46 Nm/kg maximum torque in the knee for young, healthy individuals at self selected speeds (Momcilovic, 2010).

2.3.2   Ascending and Descending Stairs

Ascending stairs is a cyclical process that engages muscles throughout the body, but as people get older, knees become one of the biggest factors in one's ability to do so.

To understand the role the knee plays in stair ascension, it is important to define clear stages in the cycle. The ascending stair gait cycle is split into the stance and swing phase. These phases are characterized by specific lengths of time. The stance phase makes up about 66% (slightly varies depending on the person) of the cycle and includes weight acceptance, pull up, and forward continuance (Komistek, Dennis, & Mahfouz, 2003). The swing phase consists of foot clearance and foot placement and makes up about 34% of the cycle (Komistek et al., 2003). A visualization of this is in figure 6.
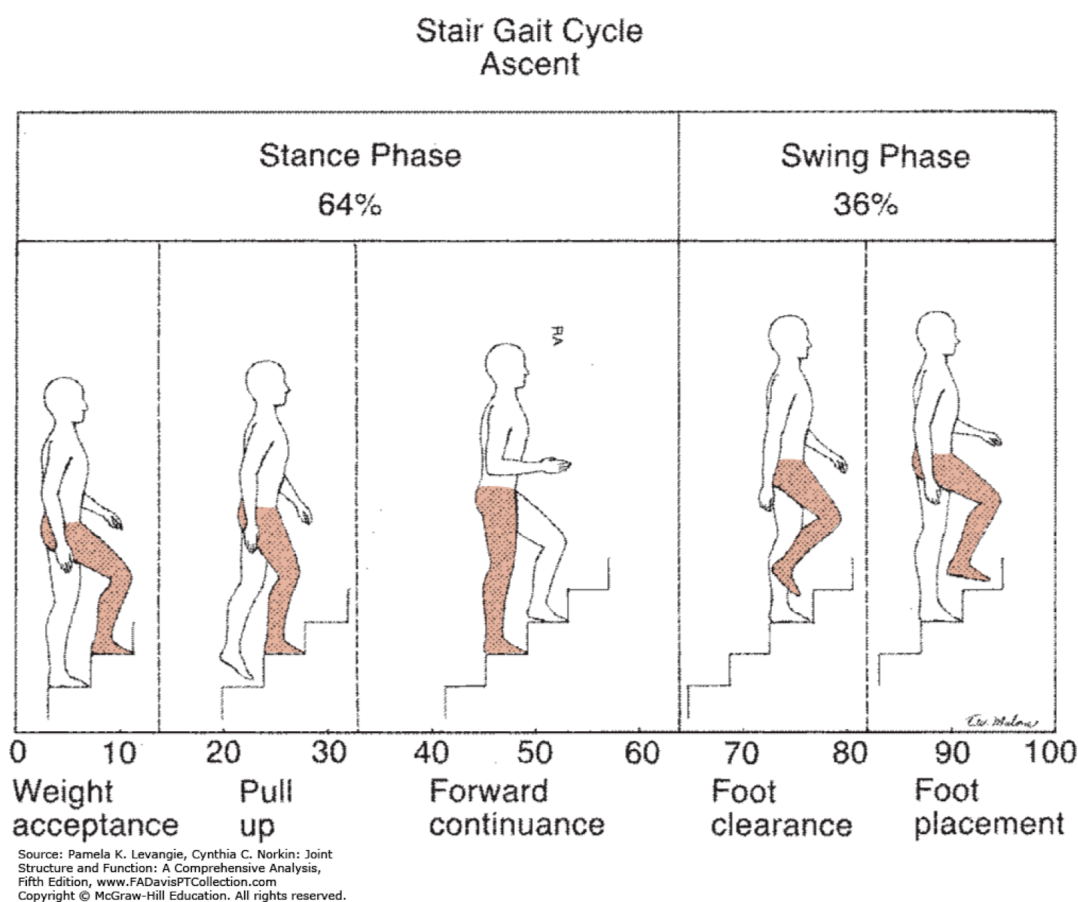
Figure 6: Gait Cycle of Ascending Stairs, adapted from (Olney & Eng, n.d.)

The knee is most active in the initial stance phase, when the knee muscles are involved in driving one up and down stairs. From this point until the next stance phase, the knee is mainly tasked with bearing the load of the body while the other leg is in the swing phase. This means that the knee will distribute the load properly to your trunk muscles. During this, 15 different muscle groups are activated. The process of walking upstairs can be broken down into further subtasks, but is best understood in a general sense as these

2 phases divided into 3 and 2 sub-phases respectively (Abbas & Abdulhassan, 2013). During stair ascension, the average normal force exerted on the knee is about 316% of a person's total body weight (Kutzner et al., 2010). Alternatively, there is a descending stair gait cycle. It also consists of two phases: the stance phase and the swing phase. The stance phase makes up 60% of the descent gait cycle and includes weight acceptance, forward continuance, and controlled lowering (Komistek et al., 2003). The swing phase makes up 40% of the gait cycle and consists of the leg pull through and foot placement (Komistek et al., 2003). A visual of the descending stairs gait cycle is shown in figure 7.
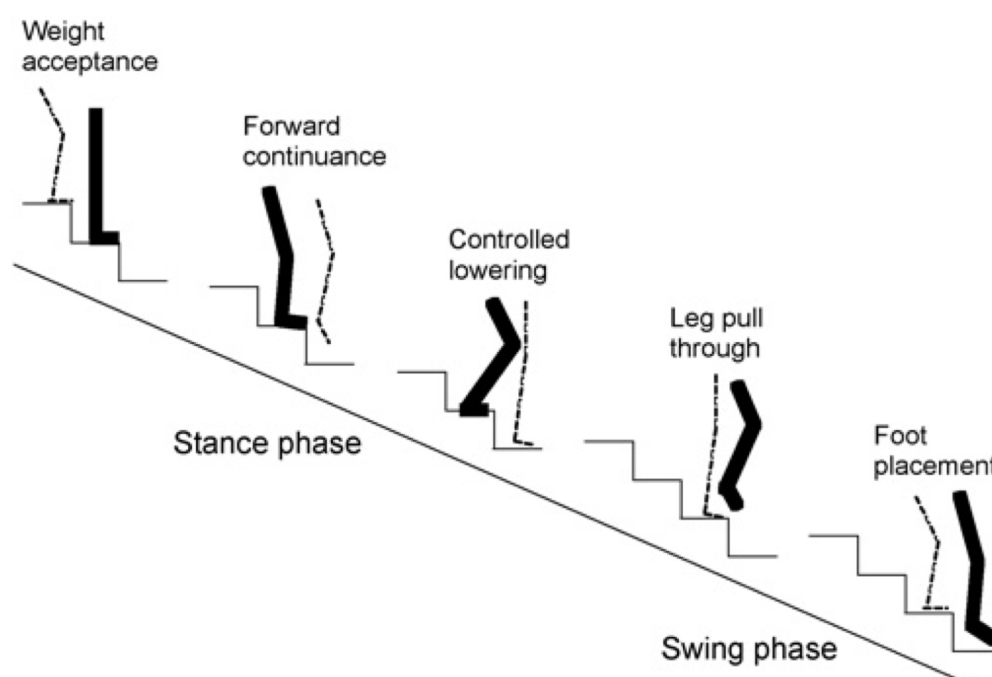
Figure 7: Gait Cycle of Descending Stairs, adapted from (Novak et al., 2010)

The average normal force exerted on the knee while descending stairs is about 346% of a person's total body weight (Kutzner et al., 2010). This is a slightly larger force than that of stair ascension and a much larger force compared to that of normal walking. With the basic gait cycle understood, a full analysis of the knee joint and its variables must be conducted. Firstly, it should be understood that these variables are affected by different heights, weights, ages, environments, or even mental health. This is evident when taking into consideration that a taller test subject will have slower joint velocities than a shorter subject since they have longer legs (Adiputra, Parasuraman, Khan, &

maxon

Elamvazuthi, 2015). The knee muscles must also provide more force in a heavier subject than a lighter subject. In general, going down the stairs requires more of a reactive force than going up the stairs, and going up multiple flights of stairs will require increasing amounts of force since the subject's muscles will fatigue (Abustan, Ali, & Talib, 2018). Combining these variables leads to a significant range of required forces to move the knee joint during stair ascension and descension. Fortunately, the knee joint has only one degree of freedom which has a range of 125 degrees itself, making it slightly easier to isolate forces than other joints such as the shoulder, wrist, or ankle - all of which have multiple degrees of freedom (Frisch & McClure, n.d.).

The maximum joint force during the stair gait cycle is three times the body weight. The approximate overall flexion moment during stair ascension is 2.29% BWm and that for stair descension is 3.16% BWm (Kutzner et al., 2010). This is approximately a 0.98 Nm/kg maximum torque in the knee for stair ascension in healthy individuals at self selected speed (Momcilovic, 2010).

3 Goals

This team's central focus was to design an assistive device able to actively help someone with a weakened knee; however, the project goals have evolved over time. Initially, the team had aspirations of creating a slim device capable of providing a torque approximately 10% of the average person's body weight. Existing active knee devices provide a much larger body weight percentage of assistance, but this project sought to create a relatively inexpensive device for those that desire non-intrusive assistance.

Over the course of this MQP, the goals have shifted slightly due to constraints lack of available with machining equipment, and restrictions put into place by COVID-19. The team originally planned to machine their own gears to achieve a higher torque to speed ratio. Unfortunately, Washburn Shops did not have the equipment to produce small gear features, so the only gears available were in undesired sizes and materials. A time constraint example encountered was the lead times for the outsourced parts, such as the gearing and motors. Due to all of these physical constraints, the team was unable to fully manufacture the hinge subsystem before COVID restricted access, but an idealized version of the design was created in SolidWorks. The idealized version exhibits a device that is slim and provides enough assistance without needing to compromise on various constraints.

4   Methodology

The methodology will discuss the development process of the active knee device through three different sections: mechanical design, biomedical design and test procedures, and actuation of the knee.

4.1   Mechanical Design

4.1.1   Phase One: Design Ideation

The early stages of the design team's product development process involved hand-made drawings that described the appearance and functionality of the device. The team discussed various potential energy solutions to support its goals to provide force to the knee joint including hydro muscles, a motor, cables, and springs. Due to the interdisciplinary nature of the group, using a motor to actuate the device best emphasized each team member's strengths. The motor allows the team to fully control the movement of the device and provides a way for other components to easily interact with the actuation. In conjunction with the motor, the design incorporates an electromyograph (EMG) to identify the user's movement and controls the motor movements. The team decided to use a planetary gear system to reach the determined torque because of its compact design. The motor input will rotate the sun gear, which will turn the planetary gears (Kaim, 2000). The evolution of this device, detailed in the following section, is shown through the different conceptual models. Following the drawings, multiple SolidWorks iterations were created and the final version was manufactured.

4.1.2   Phase Two: Design Optimization

Design Evolution

The following figure 8 is a time-line in terms of design evolution. The first drawing portrays the active assistive knee device's earliest potential design. It utilizes the idea of a 90% nylon sleeve to protect a user from the skin to machinery contact. This sleeve, which feels similar to legging material, is slightly compressed to hold its placement on the

maxon
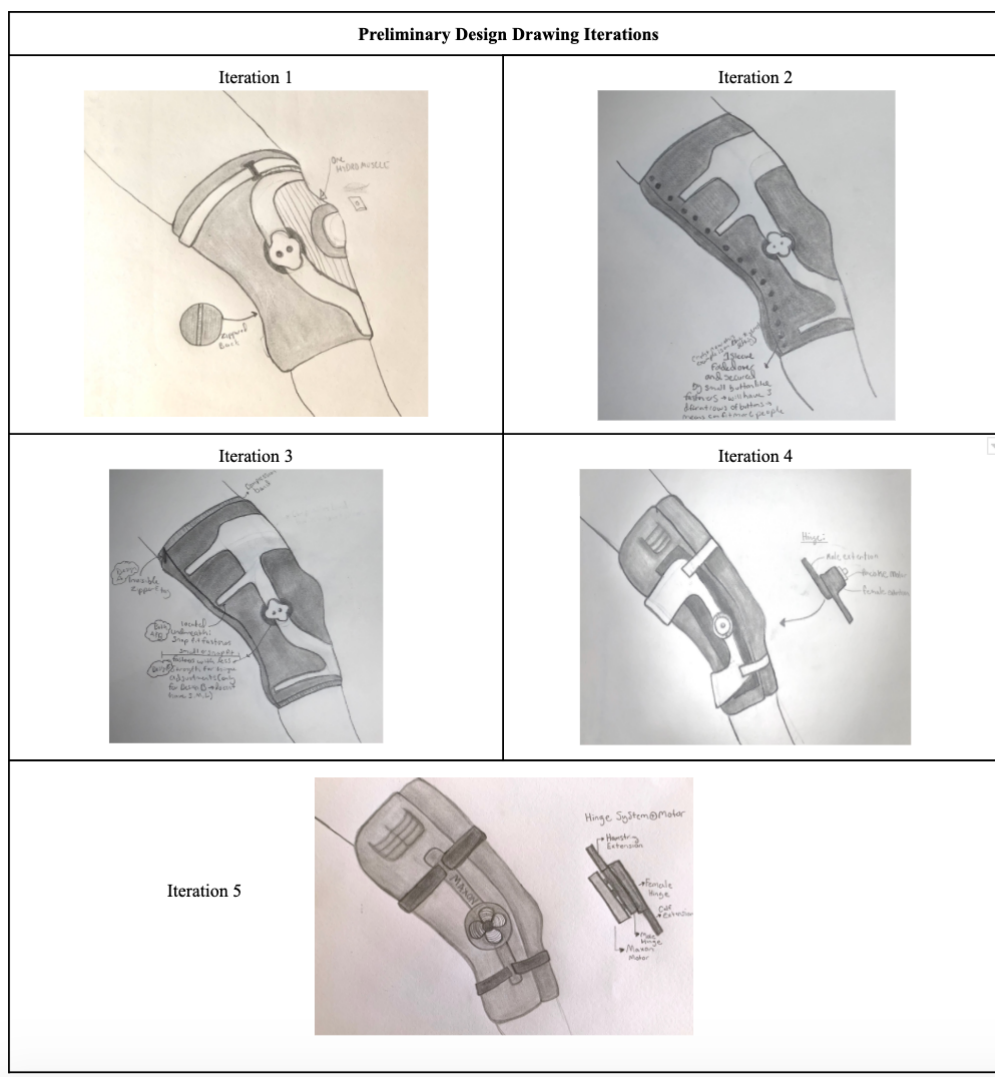
Figure 8: Drawing Iterations

knee. While the protective sleeve idea has stayed consistent with the final design, features in iteration one, such as hydro-muscles, were dismissed. Improving the application to a user's leg was focused on in the second and third iterations. The second drawing illustrates fastening buttons vertically down one side. The sleeve would have multiple snap fasteners at different diameters. This idea seemed reasonable because it made the device adjustable for a range of unique leg size and easier to put on. Similarly to the fastener idea, the third iteration used zippers in different diameters that would allow a user to adjust to their desired sleeve compression. Another feature change to the second and third iteration was removing the upper and lower extensions projecting off of the hinge system. The extensions wrap around the front half of the lower hamstring and upper calf, which are

rigidly connected to the hinge to support the bending motion created by the hinge's motor. The team realized that these extensions must wrap behind the leg to better support the assistive motion produced by the energy of the motor, which can be seen in the fourth image. The hinge system was also adjusted to be a snap-fit, which was later changed. The final image was created after SolidWorks modeling was completed to give a realistic image of the system as a whole. In the fifth drawing, the hinge system is covered by the motor and the extensions become vertical posts on the leg's sides to the lower hamstring and upper calf muscles. At the end of each extension, they have two rectangular holes meant for elastic bands and Velcro hook-and-loop to wrap around the leg to hold the extensions in place. This hook-and-loop would be adjustable for the user and would have a rubber lining on the outside (attached to the nylon sleeve) to further increase friction to prevent unwanted slipping. This design also takes advantage of the adjustable zipper idea from iteration three to make it easier for users to attach the device to their leg.
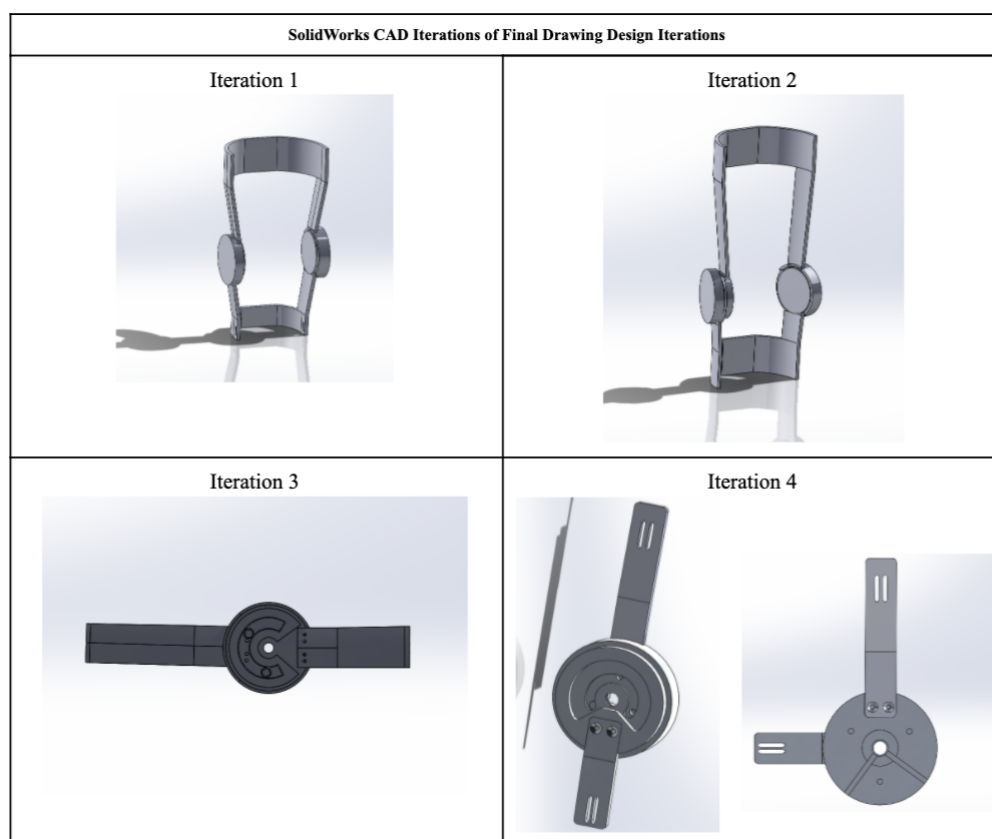
Figure 9: SolidWorks 3D Model Iterations

Figure 9 demonstrates the progression of this assistive device's 3D models. The first 2 iterations appear similar because they carry the same snap-fit hinge system. The design team believed that using the average diameter size of a humans lower hamstring muscle and upper calf muscle would make the device fit a larger range of people. It also used slight angles from the hinge to extensions to provide a tapered shape to fit the natural incline of a human leg. The second iteration played with increasing the hamstring extensions height to provide the user with more support. The hamstring height was decreased back down to 8 inches from the knee to reach the device's total sleeve length constraint of 16 inches. The team believed perfecting the right shape and dimensions of these wrap-around extensions would take a long time and many physical prototypes to perfect, so they were removed and replaced with holes for Velcro hook-and-loop. This made the device more universal for future testing. The third photo in the chart shows a dramatic shift in the hinge system. The robotic team's motor research proved that a motor within the team's size and power did not exist. This constrained the design team towards implementing a planetary gear system to increase the amount of torque being produced. The hinge now uses pegs from the female hinge going through the male hinge's horseshoe shape. These pegs hold the planetary gears in place by fastening with shoulder collars on the inside of the male hinge's cavity. The final iteration depicted above, shifts away from the shoulder collars to shoulder screws.

Manufacturing Process

After the design of the device was finalized for prototyping, the team moved to producing the physical device. First, tolerances needed to be adjusted to the final CAD model. The design team created the chart below, noting each feature and their relation to each other. The tolerance table seeing in table 1 helped organize the type fit to follow and the value range required to be input into the model's dimensions.

After researching, the team decided to use 6061-T6511 aluminum because it is light and cheap, allowing for the team to make multiple iterations. The team ordered two 5"x5"x2" aluminum blocks from Peterson Steel Company, a local business in Worcester,

maxon

Tolerancing of Demo CAD for Manufacturing

Part or Feature:	Tolerance Type Fit:	min/max
Male Hinge: extensions cut extrude to fit extension	Locational clearance	Dim: 30 mm Min: 29.986 Max: 30.021 Mid-Range Dim: 15 mm Min: 14.989 Max: 15.018 Mid-Range: 0.0145
Male Hinge: screw holes for extension	Sliding Fit close fit, metric tap & clearance drill sizes (do drill sizes)	*h9/d9, H9/D9 For M5 - 4.2 as drill size
Male Hinge: Ring gear fit into male hinge	Force or Medium Fit	Shaft Dimension: 90 mm Min: 89.907 Max: 89.942 Mid-Range: 89.9245
Female Hinge: motor holes/screws	Sliding Fit Through holes for M5	Min: 4.188 Max: 4.212 Mid range 0.014 Made it 5.35 because the screw thread is smaller, it should slide through easily
Male Hinge: screw holes for shoulder screws	Sliding Fit for M5	4.2 for Drill size Mid range 0.014
Male Hinge: Motor hole	sliding/close-running	Shaft Dimension: 10 mm Min: 10.013 Max: 10.035 Mid-Range: 10.024

Table 1: Tolerance Chart

MA. Unfortunately, the manufacturing process took the team longer than anticipated, due to the fact the team needed lab assistance to properly use the manufacturing equipment. Over multiple weeks, the team met with WPI staff to consult and learn ESPRIT, a computer aided manufacturing (CAM) software, and a Haas Mini Mill, a machine used for subtractive manufacturing. Originally, the design included multiple extrusions for the planetary gears to mount on. The team switched to using shoulder screws to mount the gears on, simplifying the design, and making the machining easier. When the team manufactured the male hinge, they didn't compensate for the tool's diameter, which can change over time. This resulted in the male and female not fitting together properly, so they had to re-machine the male. To machine the hinge subsystem, the mini mill would remove the excess material and shape it into a cylinder. Then the machine would create a pocket in which it would drill several holes, one for the motor shaft, three to mount

maxon

the motor, and two more for to attach the extensions. Machining the top of each block left a big rectangular extrusion on the bottom of each cylinder. To remove that material, the team had to create soft jaws so the machine could hold the circular shape of the hinges while facing off the material on the other side. Progression of manufacturing was brought to an abrupt end due to COVID-19. This team was unable to get onto campus during D-term and finish the minor manufacturing changes that required the resources of Washburn Shops. Figure 10 and Figure 11 show the progress of the male and female hinge parts.

Figure 10: Manufactured Male Hinge
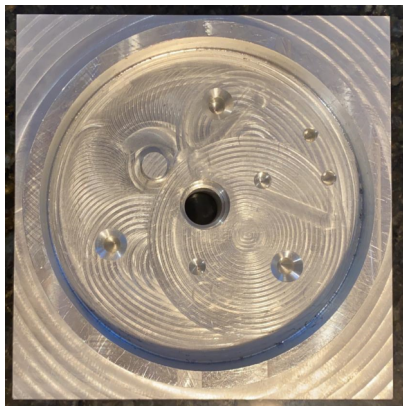
Figure 11: Manufactured Female Hinge

4.2 Biomedical Design and Test Procedure

4.2.1 PracticePoint

A literature review and a live model motion capture using WPI PracticePoint's Vicon motion capture system were conducted in order to accurately depict the amount of force

required to assist the user during stair ascent and descent. The team hoped to test both young subjects as well as elderly subjects such as Professor Guceri; however, due to time constraints as well as lack of access to the lab, it was only possible to test young, healthy subjects which consisted of members of the team.

Once the team gained access to PracticePoint, a set of stairs was created - dimensioned to fit PracticePoint's force plates of the motion capture system. These stairs can be seen in figure 12.
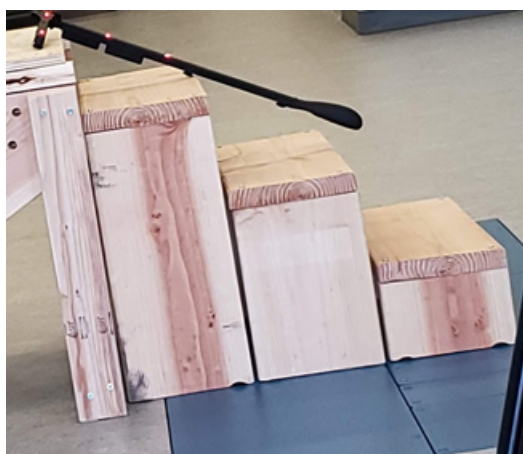
Figure 12: Stairs used in PracticePoint. Image taken during calibration.

The motion capture system measured the subject's knee forces while ascending and descending stairs. The goal was to observe the difference in torque measurements between the subject walking up and down the stairs. The measurements occurred at the beginning of the project to gather necessary data, as well as at the end of the project when the device was completed. This allowed the team to measure the effectiveness of the provided assistance for the subject.

PracticePoint's motion capture system was calibrated by inputting body measurements and calibrating the cameras. SACR markers (reflective fiducial markers) were placed on the subject in the locations directed by the Vicon full body modeling with plug-in gait (Vicon, 2020). This arrangement can be seen in figure 13. Once the markers were placed, the subject walked up and down the stairs that were on the force plate. The visual representation along with the pressure from the force plates were recorded in order to measure the force, position and rotation of the knee during the desired activities. This

can be seen in figure 14.

Figure 13: Testing at PracticePoint

Figure 14: Testing at PracticePoint

4.2.2   The Electromyograph

Electromyography was first discovered in 1771 when Luigi Galvani found that electrically stimulating the muscle tissue of an animal caused the muscle to contract (Kazamel & Warren, 2017). In 1942, Herbert Jasper at McGill University created the first electromyography machine (Kazamel & Warren, 2017). The procedure uses an electromyo-

maxon

graph (EMG) to measure the speed and strength of the signals traveling in a specific muscle. This connection is created by electrical signals conducted through the motor neurons of the muscle that causes contractions. The electrode of the EMG is able to conduct these electrical signals and translate it into numerical values ("Electromyography (EMG)", 2019).

For this project, the EMG was created and used as a method to actuate the device. The EMG is a complex circuit containing multiple operational amplifiers. Figure 15 below shows the schematic for an EMG. Following this schematic, an EMG circuit was created by the team to test the muscle activity in the leg. Figure 16 shows the circuit created. This circuit was not feasible as it was quite large and ineffective. The MyoWare sensor was implemented while trying to find better ways of conducting the EMG.
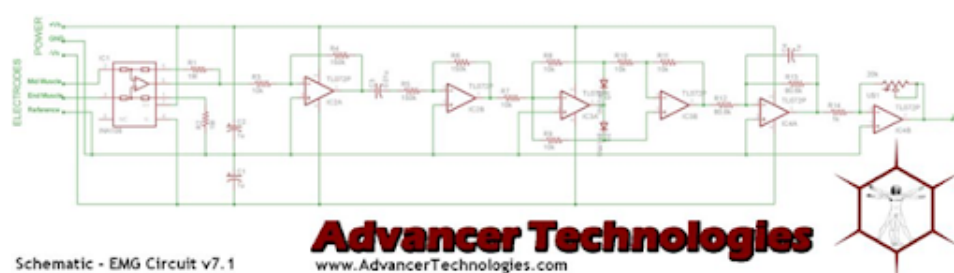
Figure 15: EMG Circuit, adapted from (Technologies, n.d.)
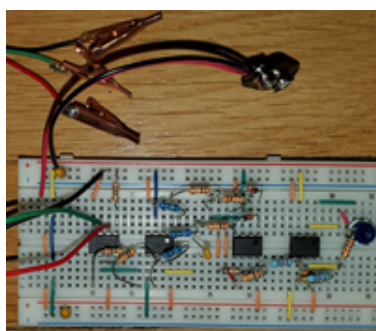
Figure 16: EMG

The MyoWare is a small EMG sensor that allows the measurement of raw, amplified, rectified, and integrated signals of the muscle activity (MyoWare, 2015). The EMG data is raw and requires further processing in order to act upon(Raez, Hussain, & Mohd-Yasin, 2006). To gather quantifiable data, the signal is rectified then integrated (MyoWare, 2015). To rectify the signal, the mean of the absolute value is taken over a certain time

period (*Automated EMG Analysis*, n.d.). The integral of this rectified signal is then taken, resulting in an integrated signal. This is the signal pictured in figure 17.
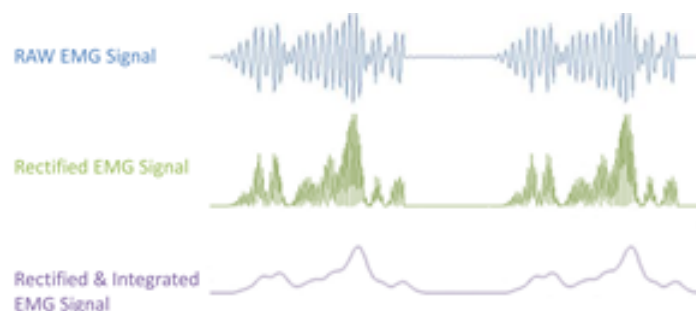
Figure 17: EMG Signal, adapted from (MyoWare, 2015)
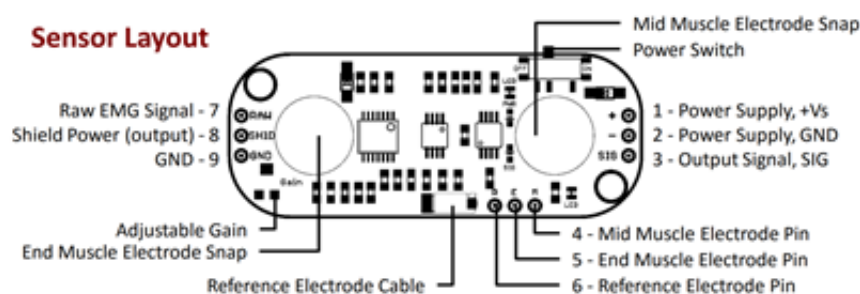
Figure 18: MyoWare Schematic, adapted from (MyoWare, 2015)

The MyoWare Sensor (schematic seen in figure 18) connected to the Feather board for a power input and the signal output. For testing, a USB isolator was connected to the Feather board to protect the human body from receiving any voltage source. This was connected to the laptop to provide power as well as read the data through the Arduino IDE program. Originally, the sensor was connected to adhesive electrodes that attached to the skin.

Unfortunately, there were connection difficulties with these electrodes in that even when tightly adhered to the skin, the signal would drop completely. The team re-soldered connections multiple times before realizing this was not the issue. Ted Clancy, a biomedical engineering department professor, advised the team to troubleshoot the problem by testing the hardware first. Troubleshooting the hardware consisted of sending a signal between 60 and 120 Hertz directly to the MyoWare sensor and reading the output signal. If the signal displayed were a sine wave, the hardware would not be at fault. After conducting the test, the students found the problem was with the connection to the human

body, not the hardware itself (Webb, 2018).

For a better connection to the skin, it was imperative that the team understood the electrode's function. The electrode is composed of metal in contact with an electrolyte as seen in figure 19. It is used to measure the ionic currents within the body that are caused by action potentials along axons (muscle fibers) by converting these currents into an external potential. This potential is created through the half-cell (metal with electrolyte) created in the electrode. The most common electrode used is the silver/silver chloride (Ag/AgCl) electrode due to its low half-cell potential. The connection between this electrode and the skin should have an impedance between 1 kΩ and 10 kΩ. To obtain this connection, the electrolytic gel allows the charges to be transferred from the tissue to the electrode. It also increases the skin to electrode contact surface and secures a better contact to the skin which reduces the contact impedance (Webb, 2018).
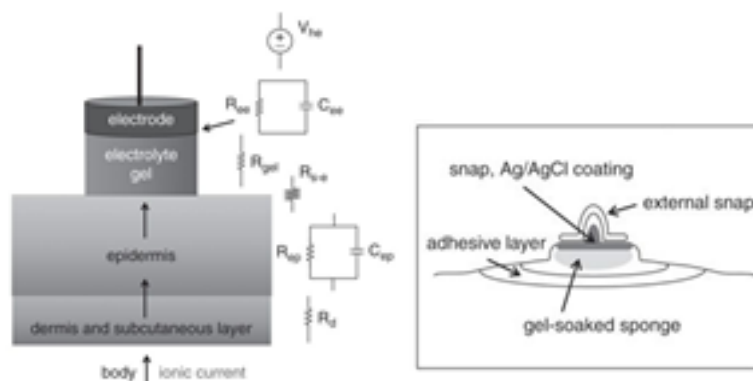
Figure 19: Electrodes, adapted from (Webb, 2018)

The team replaced the disposable electrodes with silver metal electrodes. Electrolytic gel was applied for better contact with the skin without an adhesive, and a medical wrap was used to hold the EMG. The team met with electromyography experts at Liberating Technologies. They advised the team to remove a dead skin layer with an alcohol wipe and to rub the gel into the skin to allowed for a stronger connection to the muscle activity. While this process is intrusive for a user, establishing a working model for the first prototype was critical since the EMG is responsible for controlling the motion of the device.

The experts at Liberating Technologies also advised adding a voltage follower to the

EMG circuit, since the original EMG frequently lost connecting. A voltage follower acts as a buffer to the signal, and does not change the output signal because it has no feedback resistors. It also draws minimal current because the operational amplifier has a high impedance. The EMG had a low impedance and because of this, drew a large current - causing the unstable connection between the EMG and the laptop. The addition of the voltage follower would allow the EMG to have a steadier reading; however, due to limited resources, it was not possible to add the voltage follower to the EMG (*What is a Voltage Follower*, 2020).

Because the voltage follower was unable to be added to the MyoWare sensor, the team decided to purchase a new electromyograph. Purchased though Seeed Technology and seen in figure 20, this new electromyograph was consistently functional and used in the final prototype. It includes a Grove-EMG detector, Seeeduino V3.0, Grove-LED Bar, and the Grove-Base shield. This device is intended to light up the LED bar as it senses muscle activity, and the team was able to export its data for analytical purposes (Ltd., 2020).
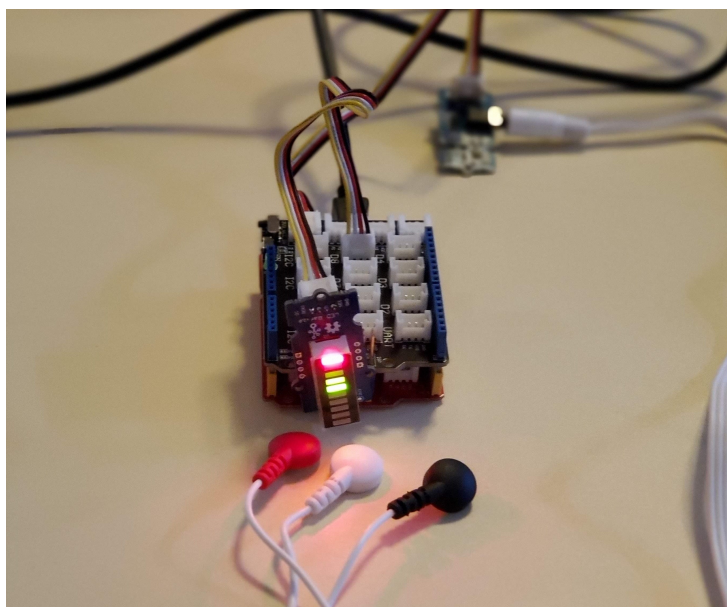
Figure 20: Final Elecromyograph

A plot of the data taken from the Seeedstudio EMG can be seen in figure 21. This plot shows the reading of the quadriceps while the subject was ascending stairs. The EMG data outputs is integrated but not rectified. The team began to implement filtering in

the code but they were not successful in completing this filtering given the time they had.
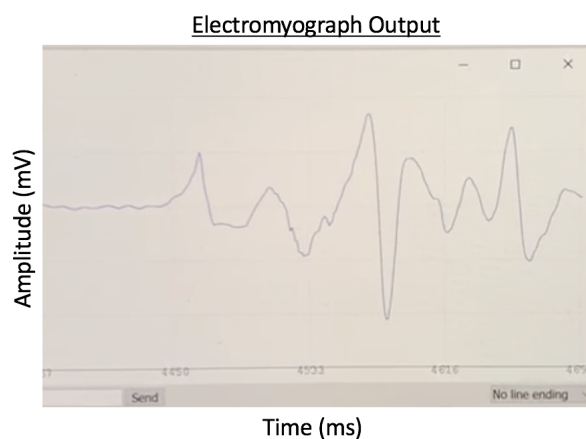
Figure 21: Signal Plot of Seeedstudio EMG

4.3 Actuation of the Knee

4.3.1 Component Selection

The major components of the mechatronic design of the device includes a motor, motor controller, and battery. The motor controller offers precision control for the position, speed, and torque of the motor during movement. In order to determine the proper specifications of a motor that would best suit this application, the team used both the aforementioned research and test results to find the average torque exerted at the knee in stair ascension and descension. From this, the team was able to determine the motor specifications under various weights, both with and without a gearing mechanism.

As evidenced above, achieving the required torque without a gearing mechanism requires a bulky DC motor, which would hamper the user. As mentioned in the gearing section, the team is gearing a 3 to 1 torque to speed ratio to avoid excessive weight. This is made possible by the low speed requirement of 80 revolutions per minute as its peak rotational velocity (240 RPM required to attain this after gearing). The calculations in table 2 are based on the literary research that identified the maximum required torque in stair ascension as 0.98 Nm/kg (Momcilovic, 2010). The team then decided that assuming the subject to be 90 kilograms (200 lb.) would take into account subjects of most sizes for testing purposes.

maxon

25

Required specifications with 3:1 gearing (90kg)			
	Total	**10%**	**5%**
Torque (N*m)	29.400	2.940	1.470
Speed (RPM)	240	240	240
Power Req (W)	738.9	73.9	36.9

Table 2: Required Motor Specifications after Gearing

Based on table 2, the team decided to use a motor with a slim profile that would attach to the knee easily called a "pancake" motor. The peak continuous torque of the motor used was slightly lower than ideal, but since the motor only needs to operate for short periods, it should be able to handle the peak load going up and down stairs. The team was thankfully able to get the project sponsored by Maxon, which allowed the team to obtain high quality, configurable motors and motor controllers. The motor selected is also able to spin freely, forward and backward, to allow for maximum freedom when the user is not actively using the device. Reference Appendix A for more information on the motor specifications.

4.3.2   Code

EMG Code

The code for the MyoWare EMG device was taken from an Adafruit online tutorial (Adafruit, 2016). The source code was a simple loop that read the analog output of the MyoWare sensor and converted it to a digital signal and printed the value. The team adjusted the source code to print the timestamp along with the digital output of the EMG. This code can be seen in Appendix C.

The Seeed Technology EMG code was also a demo code taken from Seeed studios (Ltd., 2020). This code calibrates the static position of the subject in the first five seconds, then displays the EMG reading on a scale from one to five on the LED bar. The team adjusted this demo code to print the values they needed, along with sending the voltage reading, or output, for data analysis. This code can be found in Appendix D.

maxon

Code Structure

The code was structured into a basic state machine diagram, in which each stage of the gait cycle would act as its own state. As seen in figure 22, once the EMG and encoder sense that a state has begun and ended, it will move to the next state until the subject is at rest. The Arduino microcontroller handles the logic of the sensing data and converts it into data for the motor controller to use.
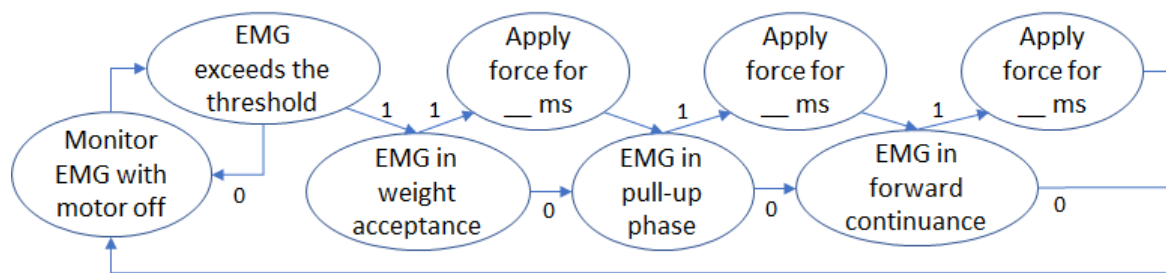
Figure 22: State Machine Structure

When the motor acts on the subject, it will do so mostly at low speeds with constant torque. The motor will exert a torque for a certain amount of time based on the user's need. If the user is weaker, the device will provide more torque; if they are stronger, the device may only provide a small jolt at each assistance point. These times and conversions based on the EMG readings will require extensive testing to ensure the user is not getting excessive or insufficient assistance. Further improvements could include concurrent monitoring of the EMG to determine when the assistance is truly unneeded instead of basing it on time, however this would add significant complexity to the program design.

4.3.3   Safety Factors

The device is designed so that it would "follow" the user's leg movement; this would reduce the torque required by the user's knee. It is not meant to overtake the individual or cause them to follow the device's actuation. To accomplish this, the EMG would sense that the user is applying a force to the knee and attempting to move up the stairs. After sensing this, the device would provide the user with the necessary assistance.

maxon

To ensure the user's safety, the device will feature an emergency button to cease all actuation and allow the device to freely rotate. This will account for any flawed EMG signal interpretation or an irregular gait. It will also prevent over-extension in either direction. The button may also be required if the speed of the motor is too fast for the user, in which case it will need reprogramming.

As previously mentioned, the program will exist in states and be cyclical. In that sense it should be highly accurate, however there could exist issues if the subject has an irregular gate cycle. A solution to this issue could be solved via an interrupt that checks if the angle of flexion has exceeded the boundary. If the boundary is exceeded the device should allow free rotation until the weight acceptance state is recognized again.

In addition to control safety factors, there are also mechanical safety factors put in place to reduce injury to the user. The mechanical stop reduces the user's knee flexion and extension, thereby reducing injury caused by overly flexing or extending the knee. Elastic bands are also used to incorporate compliance in the device. They give the user more freedom of movement and create a smoother movement for the user's leg by reducing the impact if the motor were to have a sudden jolt. This added safety feature will also help the device "follow" the human, as stated previously.

5   Experimental Section

5.1   Mechanical Testing

Unfortunately, due to COVID-19, the team was unable to get onto campus during D-term and finish the minor manufacturing changes that required the resources of Washburn Shops. This meant that the mechanical team could not test the design. It can not be confirmed that the device would have met the requirements, as it was not possible to finish manufacturing or test the system. If possible, the team's manufactured parts would have been assembled with the other hardware. The motion and tolerances, provided by the hinge system, would have been tested. Extra caution was taken to tolerance each feature to fit together smoothly, so the team is confident only minor changes would have been necessary to make to this version of the prototype. To test the mechanical system without being able to physically assemble the prototype, the team used finite element analysis in SolidWorks to simulate the movement of the device.

The team set up a basic static analysis simulation to predict the brace's reaction when performing it's function. To represent this situation, forces were applied to the extensions and hinge to imitate the resistance of the upper leg and torque from the motor. The team simplified the interaction between body and device by applying 350N at the slot in the upper extension. Additionally, 3 Nm of torque was added to the female hinge in the clockwise direction to represent the rotation of hinge resulting from the motor. The bottom extension was fixed to serve as an anchor for the device when engaged.

As shown in figure 23, the majority of the stress is centered where the fasteners secured the lower extension to the male hinge. The largest displacement is located at the end of the upper extension and the largest strain is found around the bolts and lower extension. For a complete depiction of this process, reference Appendix E.

maxon
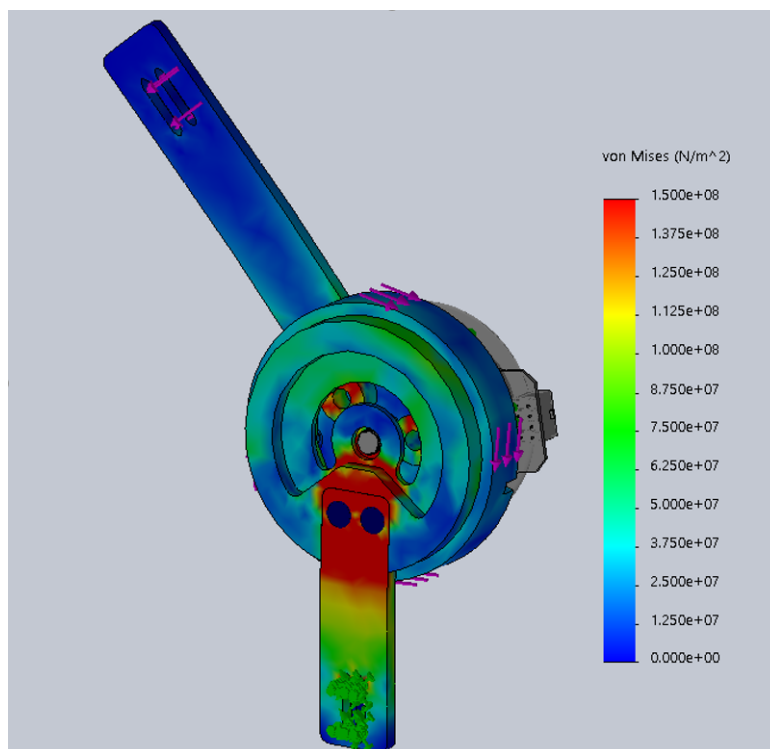
Figure 23: SolidWorks Stress Analysis Simulation

5.2   Biomedical Testing

5.2.1   PracticePoint

According to a study conducted on 10 healthy subjects, the joint moments during stair ascension and descension are seen in figure 24 below (Redfern et al., 2010).
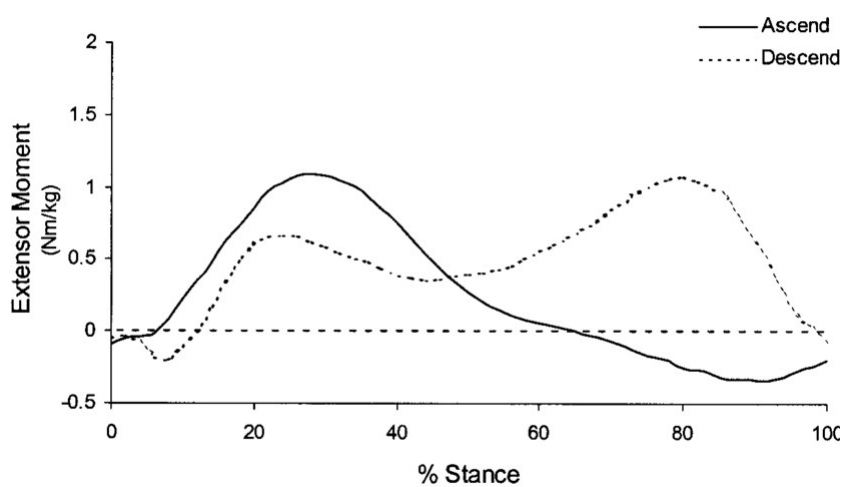
Figure 24: Moment in the knee during stair ascent and descent
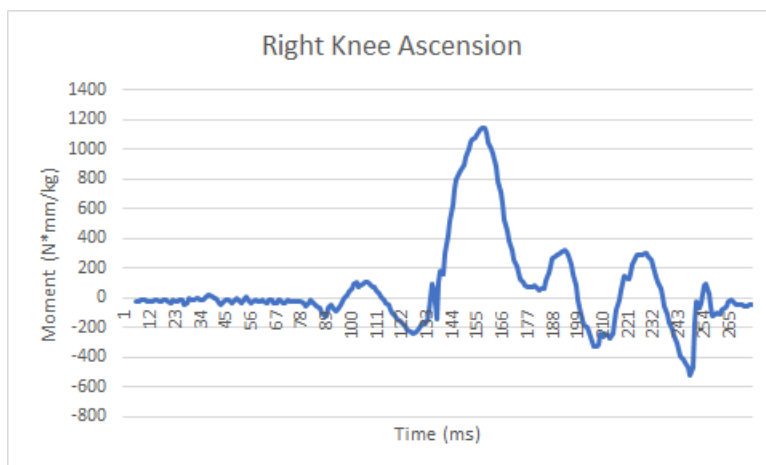
Figure 25: Moment in Right knee during Ascension

SUBJECT	Ascending (N*m)	Descending (N*m)
1	38.23	83.72
2	72.56	128.69

Table 3: Measured Torque in Right Knee

From the data exported from the Vicon motion capture system, the maximum torques during stair ascension and descension were found. After graphing the moment of the right knee (seen in figure 25 above) the maximum point of the gait cycle was identified. From this point, the torque was calculated. The maximum torque in the right knee during stair ascension and descension can be seen in table 3.

5.2.2   EMG

The team created a testing procedure to gather data on the user intent. One purpose of this testing procedure is to determine threshold values for walking, going up and down stairs, and at rest. Additional purposes are to determine the average EMG value in each stage, map the output voltage to an identifiable process in the gait cycle, and potentially identify points of difficulty or inconsistency. The EMG would be connected to the user's quadriceps, and the subject would be asked to perform several actions. The values obtained from this experiment would have been placed in a table such as table 4.

In this procedure, each subject would be asked to perform several actions multiple

maxon

Subject	Walking Range	Upstairs Range	Downstairs Range	Resting Range

Table 4: Table for EMG Data Gathering

times. For ascending and descending stairs, the subject will walk up and down a flight of approximately 6 stairs at a consistent pace and intensity. For walking, the subject will walk straight down a hallway for 10 seconds. At rest, the subject will sit in a chair for 10 seconds, and stand for 10 seconds, both recorded separately from one another. Finally, the subject will be asked to stand up from a seated position and sit back down ten times for a higher threshold value. With the collected data, the ranges and averages will be calculated for each subject. Outliers will be highlighted for further filtering.

The team intended to export the data collected from the EMG to a CSV file to analyze the data. For this, the team used a third party software called Terra Term (OSDN, 2020). Terra Term worked well for exporting the data that was collected from the MyoWare sensor, but did not work for the Seeed Technology sensor. If the team had more time, they would have been able to successfully export the data to a CSV File for data analysis.

5.3 Robotics Testing

Once the team acquired the motor and motor controller from Maxon, it had to be calibrated first to ensure accurate encoder and hall sensor readings, as well as smooth motion. Using the EPOS4 motor controller documentation, a detection test was run and the settings were applied. Figure 26 shows the regulation tuning screen; after pressing the autotune button, the EPOS4 software calibrated the motor hall sensor and encoder value by spinning it forward and backward with a test signal. This was done three times, once for each of the parameters regulated by the motor controller: position, speed, and torque.

From here, the motor is prepared to be integrated with the final hinge and EMG.
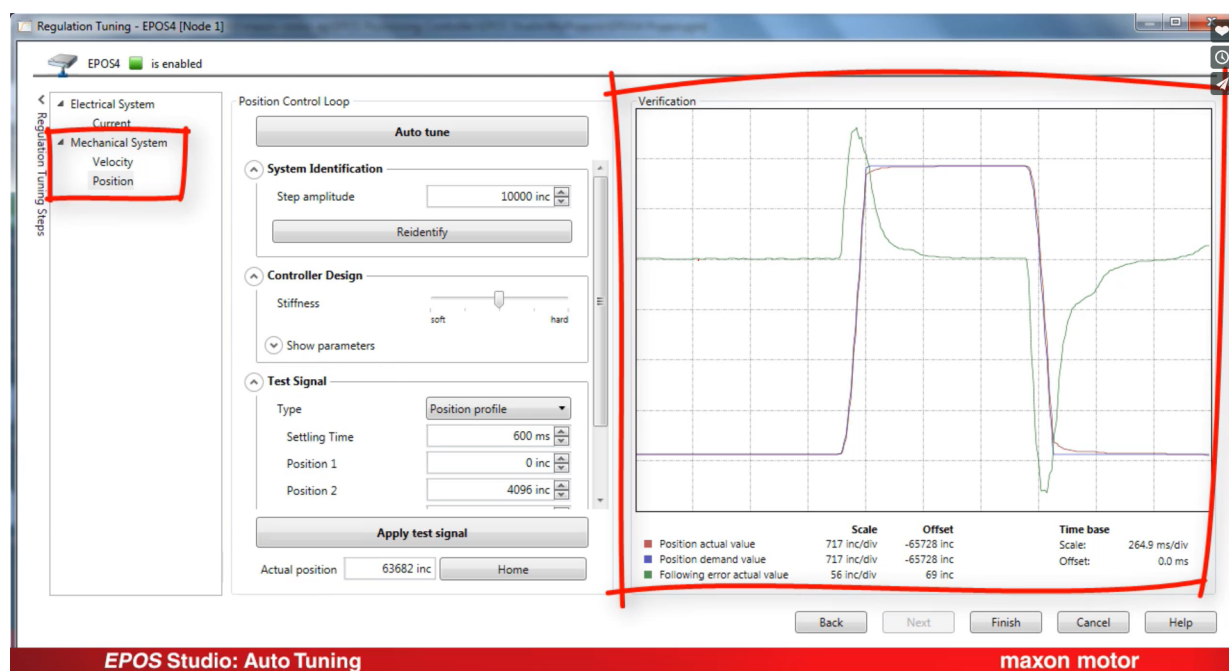
maxon

Figure 26: Motor Controller Regulation Tuning, via Maxon website (*maxon - Online Shop — maxon group*, n.d.)

Its motion will be determined by the readings from the EMG and encoder sent to the Arduino.

6   Results

6.1   Final Design

The final design of the device, seen in figure 27, is divided into five subsystems: the hinge, planetary gears, motor, electromyograph, and sleeve application. These main components of the final mechanical design are described in detail throughout this section. Outsourced materials included the two high-powered Maxon motors, 1065 Aluminum blocks, various types of screws, elastic bands, neoprene, and planetary gears. Unfortunately, the team was unable to assemble the full device for documentation due to COVID-19.

Figure 27: Final Assembly

While there is no physical prototype, the team created a SolidWorks animation representing one of the hinge subsystems. Since the video could not be shown in this paper, figure 28 depicts the different views of the device. The male was suppressed so that the planetary gears actuating the system are visible. As the system moves, the mechanical stop prevents the knee from bending over 90 degrees. Lastly, the exploded view, as seen in figure 29, shows all components of the system.
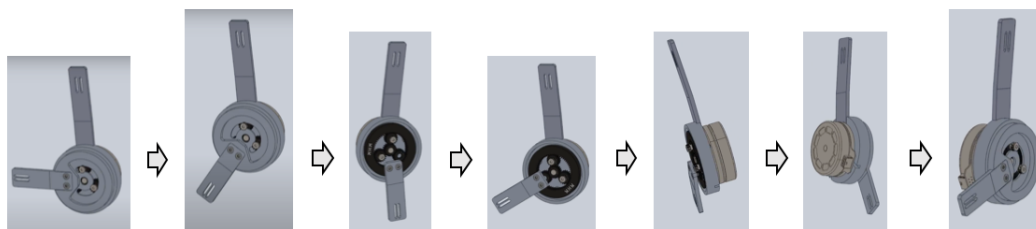
Figure 28: Animation Images
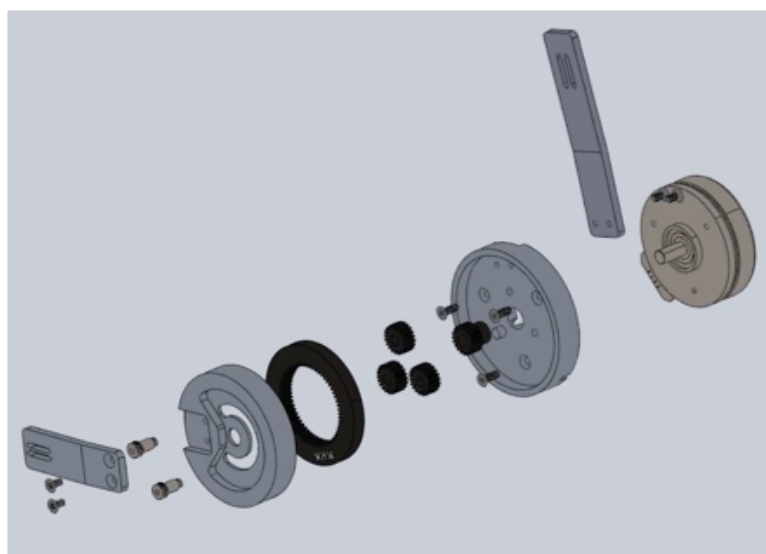
Figure 29: Exploded View

Final Design Main Components and their Features:

The Hinge Subsystem: the Male Hinge

The male hinge makes up one half of the device's hinge subsystem. It is crucial for providing housing that facilitates additional torque generation from the planetary gear system. This system is connected to the rest of the device by shoulder screws to the
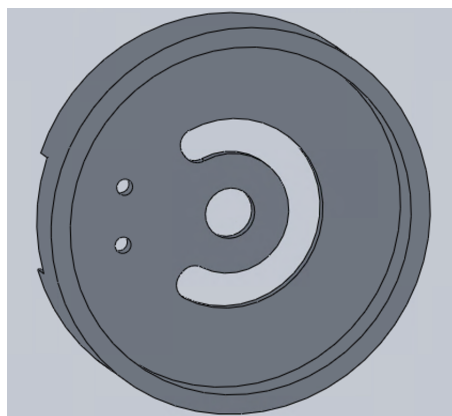
Figure 30: Inside View of Male

female, by screws through its extensions cuts, and by the motor shaft coming through the female.

A main element of the male hinge is its circular pocket, which is used for locating complimentary parts as seen in figure 30. The circular pocket is dimensioned to act as a press-fit with the ring gear and create a barrier for the other gears protruding from the female. The female hinge provides a durable and sliding housing so the male can move freely according to the torque generating planetary gear and motor system. The female's remaining planetary gears stand adjacent to the male's circular pocket. The sun gear is supported through the male and female's center hole by the motor shaft. A set screw will attach the sun gear to the motor and this will create the actuation of the hinge system.
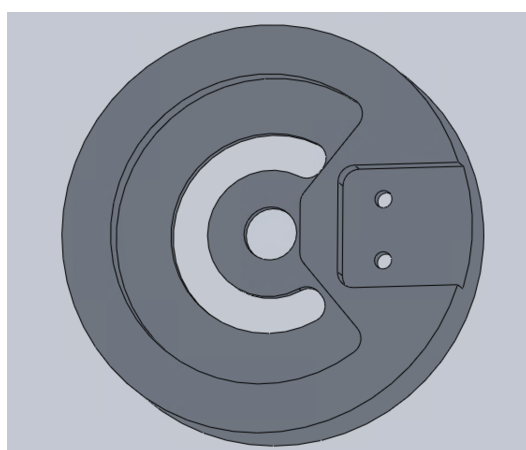
Figure 31: Outside View of Male

The opposite male orientation, in figures 31 and 32, shows the outside of the male, which would be tangent to a user's knee. The outside surface would not be exposed to a

Figure 32: Moat Cut in the Assembly

user's leg, as the protective neoprene sleeve (not shown here) will sit between the device and the skin. This side's main features consist of a mechanical motion stop, called the "moat cut," which is a horseshoe-shaped pocket and through-cut. The through-cut is offset from the pocket, and it that mimics the original pocket shape. As a mechanical motion stop, the moat cut's shape restricts a user from over-extending their knee joint, should the actuation ever fail and accidentally overextend the knee. In addition, this horseshoe "moat cut" is important because allows for the connection between the male and female. The unique horseshoe shape, seen in figure 8 and figure 32 is aligned with the circle diameter that the three internal planetary gears sit on. The three planetary gears are held in place by their "pegs" and are evenly spaced along the this diameter: one peg machined as an extrusion off of the female hinge, and the remaining two pegs are shoulder screws that go though the "moat cut." By sitting on top of this pocket surface in the moat cut, the two shoulder screws connect the male and female, hold two of the three planetary gears in place, and allow for the mechanical stop to prevent the gears from moving beyond 90 degrees.

The Hinge Subsystem: the Female Hinge

The female is the other crucial component to for the hinge subsystem. It acts as a cover and aids the torque objective by stabilizing both the planetary gear and the Maxon motor systems. Totaling to 110 mm in diameter, the female hinge is the largest

maxon

component in the system. Similarly to the male, the female is connected to the rest of
the hinge sub system via shoulder screws, screws through the extensions, and the motor
shaft.
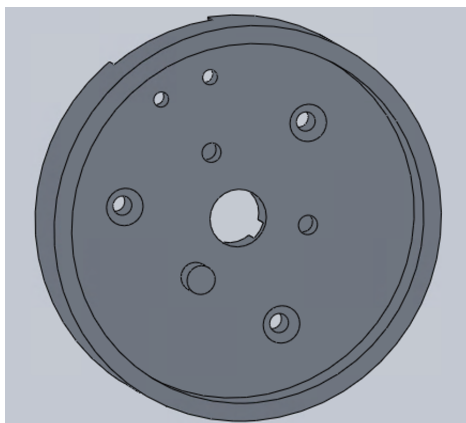
Figure 33: Inside View of Female

The female hinge's internal circular pocket, as seen in figure 11 and in figure 33, exists
as a location fit for the male hinge. Within the female's circular pocket, it holds the gear
system's sun gear, and three planetary gears against the male hinge's internal circular
pocket. The female's "pegs" are perpendicular rods that act as a central axes for the
planetary gears to rotate about. The pegs are comprised of a cylinder extrude build-into
the female and two shoulder screws.They sit on an 40 mm diameter for the planetary
gears to be aligned perfectly with the sun and ring gear, also with the shoulder screws
running through the "moat cut". Many constraints were created due to the dimensions
of the planetary gear system. In the idealized system described later, the design team
would have decreased the assembly's total size by customising gears.

The other significant feature on the opposite side of the female hinge is its back pocket
and channels (see figure 34). The 35 mm pocket exists for the location of the sun gear's
hub. The channels seen in the figure above illustrate another size constraint that the
design team faced. In order to tighten the set screw's grip, the team created 2 channels
that were 90 degrees apart from each other. These channels provide a way of fastening
the submerged sun gear hub's set screws onto the sun gear and motor shaft. In addition,
the underside of the female hinge has a cut out for the extensions to be located and
connected the hinge system.
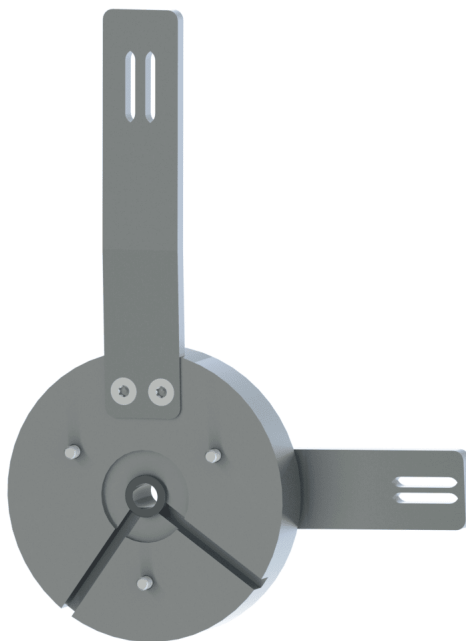
Figure 34: Outside View of Female in the Assembly

The Hinge Subsystem: the Extensions

The extensions are the last components created by this team for the device's hinge subsystem. These extensions direct a user's knee joint by the suggested motion of the electromyograph and actuation of the Maxon motor. They are attached to cut extrudes on the opposite ends of male and female hinge by screws in relation to a standing position and the mechanical stop.
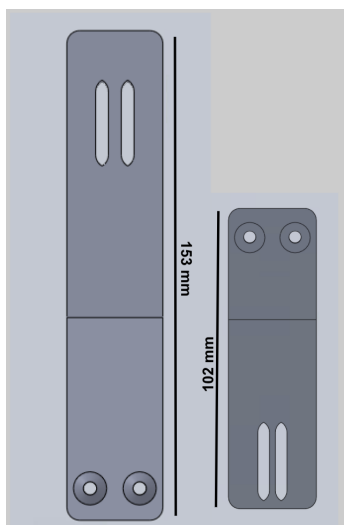
Figure 35: Hamstring Extension VS. Calf Extension

Figure 36: Extensions in the Assembly

There are a total of four extensions per device: the upper ("hamstring") and lower ("calf") extension for both sides of the leg. Figures 35 and 36 depict a front view of a hamstring next to a calf extension and the pair in the assembly. The hamstring extension is visibly longer than the calf extension because it requires more power to be generated from this muscle to move the system. Four different extensions exist is the whole leg system that needs two hinges, and two extensions are provided for each individual hinge subsystem (one hamstring extension and one calf extension). Both of the hamstring extensions are different because they are slightly bent to account for the natural taper of a user's legs. These angles are under 10 degrees and occur approximately halfway through the hamstring extension's total length. These extensions require opposite bending directions during manufacturing to mirror each other over the device; meaning, the angled portion provided to one extension would be relocated on the other side of the device but in the opposite direction. Similarly to the hamstring extensions, the calf extensions are the same length as each other, and have slightly opposing tapers.

maxon
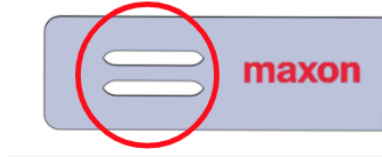
Figure 37: Slits for Extension's Wrap Around Material

Double oval shaped slits exist throughout the length of each aluminum extension. These oval cuts occur 3 times on the 8th inch hamstring extension, and twice on the 6th inch calf extension. These cuts exist to weave an adjustable elastic fastener though hinge system to the user's neoprene sleeve. See figure 37 for one instance of these slits on the calf extension. This securing material will be strong, semi-stretchable elastics bands that placed throughout these openings to secure the device to the user's leg. The elastic bands utilize a sticky rubber lining to restrict a jagged movement potentially caused by the device. Although the extensions are connected to the hinges by screws, the team wanted to enhance the system's design strength by welding the calf and hamstring extensions onto their respective male and female hinge's locations. As an homage to the project's sponsors, the Maxon Group, their logo was inscribed onto the system's calf extensions. Unfortunately, the team was unable to finish manufacturing and further look into this opportunity without access to Washburn Shops due to COVID-19. SolidWorks drawing files can be found for all the main components listed above in Appendix E.

Planetary Gear Subsystem

The final design included a planetary gear system. A planetary gear system, when compared to a standard gear system, can be much smaller and generate more torque. As a result, the wear of the engaged gear teeth is divided equally between the planetary gears, resulting in a longer lifespan (Kaim, 2000).

$$GearRatio = \frac{N_{driven}}{N_{driver}} = \frac{z_{ring}}{z_{sun}} = \frac{60}{24} \tag{1}$$

Due to stock inventory and time constraints, the team was limited in their choice of gearing as well as the producer of these gears. After researching potential companies

maxon

Figure 38: Planetary Gear system Parts within Female hinge

that would sell the required gears, the team concluded that Kohara Gear Industry was the best candidate because of their availability of stock gears, their quick lead time on customized gears, and their fast shipping. These durable parts include a ring gear, sun gear, and three planetary gears. In this design, seen in figure 38, the sun gear sits upside down in the female hinge pocket. The sun gear's hub is fastened to the motor shaft with a set screw. One planetary gear sits on a peg manufacturing into the female hinge, and the final two planetary gears held in place by shoulder screws. The ring gear is press-fitted into the male hinge's largest circular pocket. The planetary gears orbit around the the sun gear within the diameter of the ring gear's teeth. Based on the design of the device, the team needed to order a customized sun gear that could fit the 10mm shaft of the motor by utilizing a set screw.

To create a planetary gear system, there are three conditions that must be fulfilled: number of teeth on the sun gear(Za), number of teeth on the planetary gears (Zb), number of planetary gears (N), and number of teeth on the ring gear (Zc) (Kohara Gear Industry, 2015).

$$Condition(1): Zc = Za + 2Zb \tag{2}$$

$$Condition(2): \frac{Za + Zc}{N} = Integer \tag{3}$$

$$Condition(3): Zb + 2 < (Za + Zb)sin(\frac{180}{N}) \tag{4}$$

The team's current planetary gear system includes 3 planetary gears, 20 teeth each, a sun gear with 20 teeth, and a ring gear with 60 teeth. The sun acts as the driving gear

while the ring gear is the driven component. The planetary gears are fixed, but are able to rotate freely allowing for the ring and sun gears to connect. This results in a gear ratio of 3:1.

$$Condition(1) : 60 = 20 + 2(20) \tag{5}$$

$$Condition(2) : \frac{20 + 60}{20} = 40 \tag{6}$$

$$Condition(3) : 20 + 2 < (20 + 20)sin(\frac{180}{3}) : 22 < 34.641 \tag{7}$$

Maxon Motor Subsystem
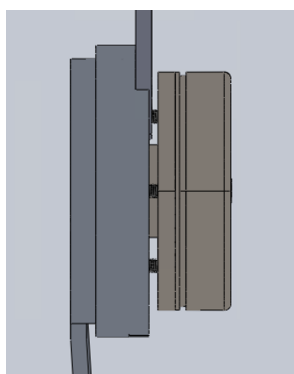
Figure 39: Maxon Motor Mounted to the Female Hinge in 3D Model
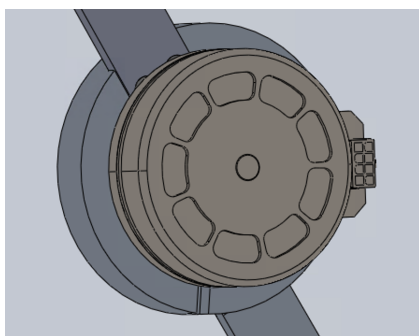
Figure 40: Maxon Motor Side View In CAD

The team was provided with two high powered motors to actuate the system provided by their gracious sponsors, the Maxon Group. The motor actuates the system by rotating

maxon   43

the planetary gears that then rotates the hinge system. It's power provides enough torque to the system in tandem with the planetary gear system to achieve the desired 10 Nm of force. In one hinge subsystem assembly, a single Maxon motor would be mounted on the outside of the female (see figure 39) and connected to the planetary gear system's sun gear with a set screw tightened on the motor shaft. Extra support to stabilize the motor was provided with three flat-head screws running through the female hinge into the motor. Unfortunately due to height constraints of the planetary gears and dimension requirements of the hinge subsystem, the motor slightly hangs off the female hinge by 3.4 mm, as seen in the figure 40.

Electromyograph Subsystem

An electromyograph was used to monitor the muscle movement within the quadriceps to command the actuation of the device and provide torque to the system. This EMG, explained in the biomedical section, attaches an electrode to a user's quadriceps. The electrode detects when a user is walking normally or ascending/descending stairs, and it will send the muscle signal data to the motor via wires. With this signal, the motor will direct the device's movement to aid the user's specific need. If the team has been able to fully assemble the mechanical parts with the EMG and motor, the rest of the electromyograph subsystem would have been located within a hand-sewn pocket on the neoprene sleeve. Small holes would be created in the pocket to allow wires connecting the EMG with the motor and with its electrodes. While being held in the sewn pocket, the EMG would not be able to move or be damaged. This can be seen in figure 41.

Sleeve Application Subsystem

The sleeve application subsystem adheres the full assembly to a user's leg and contains the device's different components. Figure 41 was produced to help a reader visualize the vision of the device's full assembly. This depiction highlights the sleeve application subsystem. The neoprene sleeve subsystem exists to increase comfort and safety for a user. This compression sleeve will act as a protective boundary layer between the user's

maxon
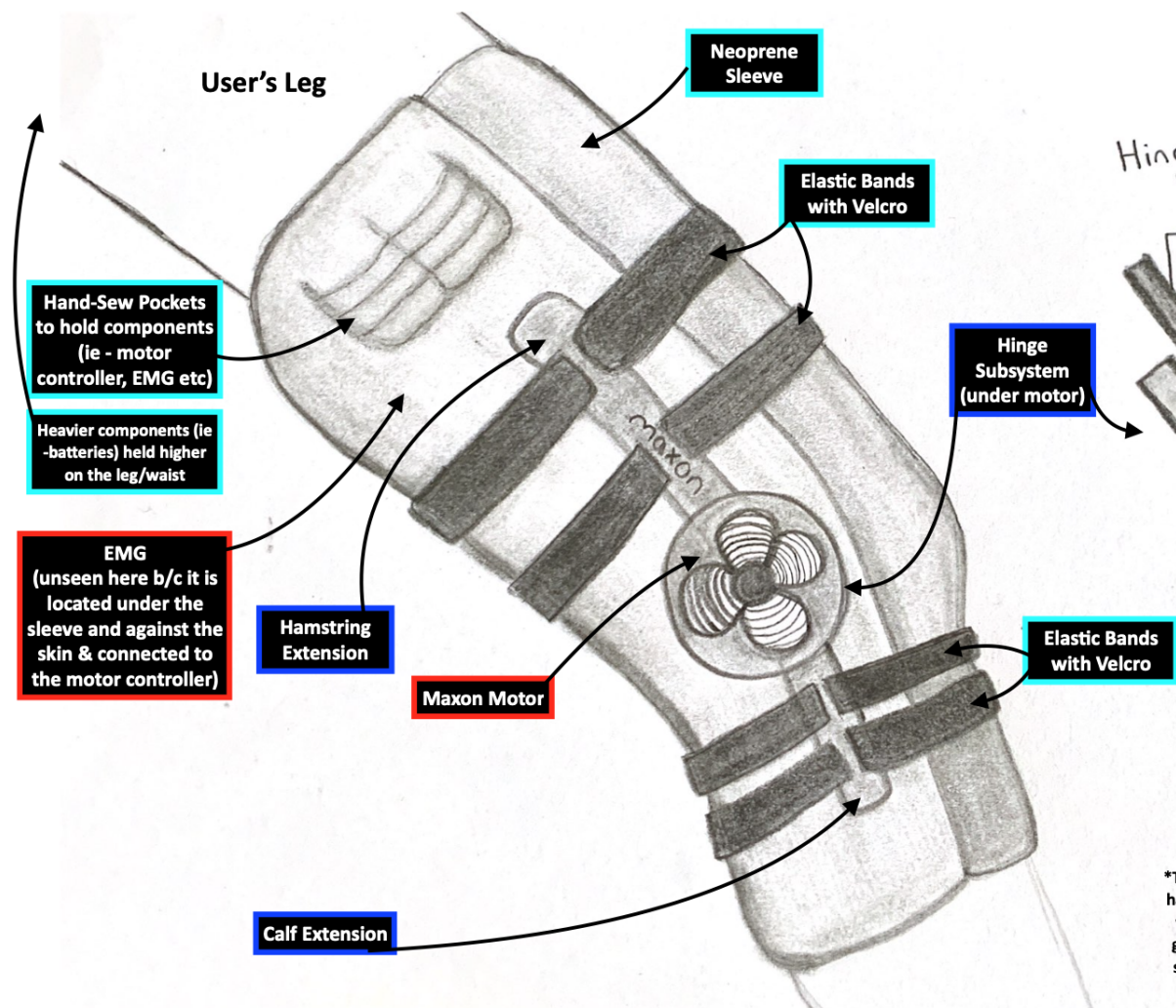
Figure 41: Sleeve Subsystem and Other Subsystems on Leg

skin and the device's different mechanical and electrical components. For the prototype, leggings (90 percent neoprene and 10 percent cotton) and zippers were purchased. The team horizontally cut approximately 16 inches of the legging's region north and south of the knee. Then, a vertical cut was made along the seam, and a sewing machine was used to attach the zippers. This sleeve had two neoprene layers, and hand-sewn pockets for holding electrical components such as the EMG and motor controller. The sleeve has 3 vertical zippers at different diameters, so a user could adjust it to their comfort compression and leg size. The device was to be put over this sleeve and held in place by the elastic bands, that used rubber to attach to the neoprene cover. Due to COVID-19, the team did not reach the final step of assembling the hinge and sleeve subsystems. The design team estimates that if assembly was completed, different methods to increase the

adhesion of the sleeve to the leg would be needed. The figure above depicts the design team's vision for the sleeve's application to the leg with its other integrated subsystems.

Idealized Model of the Hinge Subsystem

As previously stated, the team created an idealized hinge subsystem CAD model due to the constraints encountered during the design process. Due to Washburn Shop's limited tooling and equipment, the team was unable to manufacture personalized gears. This forced the team to search for gearing companies that would manufacture the specific sizes required with a reasonable lead time. The team was limited to purchasing gears that were larger and much heavier than predicted. If the proper tooling were available or the team had enough time or money, they could reduce the sizing of the gears, making it smaller, lighter and slightly slimmer.

The idealized model can still be improved and could potentially change depending on the motor shaft used. The team was able to remove 5 mm thickness of the hinge system (a 1/5 of the original) with the idealized model. The hinge diameter was reduced from 110 mm to 32.5 mm, a little less than 1/3 of the demo model's size. Figure 42, shows a side by side comparison of the idealized and demo model with the outside diameters of the female hinge annotated. The idealized model only shows the hinge system because that is where all of the changes were made.
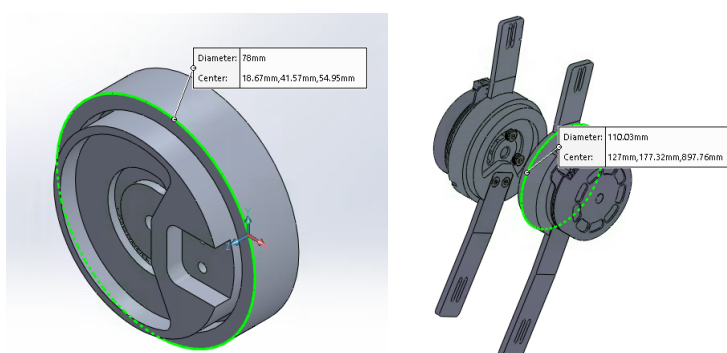
Figure 42: Idealized CAD model (left) and Demo CAD model (right) with their hinge diameters shown

maxon

7   Conclusion

Through the duration of this project, the team has developed a proof-of-concept model for the assistive device, and tested each of the major electromechanical components on an individual basis. In order to verify these components' cohesion as a whole, further assembly and manufacturing is required. Due to the Coronavirus pandemic, the team was unable to complete the manufacturing of the device, and therefore could not assemble the complete prototype.

7.1   Next Steps

If another MQP team were to further this project, the team suggests to first make any necessary CAD changes. The extensions, specifically, need some changes because the team made the decision to add more extension slots for more elastic bands to hold the device in place, however this was not implemented in the CAD models, due to the team putting their efforts toward completing the hinge system. As shown in figure 41, there are four slots on the set of extensions rather than two shown in the CAD. Ideally there would be a few more than four slots, but this figure was to show the concept of the idea. Once this change is made to the CAD model, it is recommended to finish manufacturing the prototype and assembling it. Using the prototype, they can extensively test it, to determine if the device achieves its desired function. Testing can also be done at PracticePoint to identify if the device truly provides the intended torque to the user. Other factors future teams should consider when testing include, how comfortable the device feels on the users leg, the effectiveness of the components that secure the device to the knee, the durability of the device (especially the extensions), and the adequacy of the safety precautions. These factors can provide important data such as if the device is too heavy or if it is unstable on the leg. Using this information, future groups can refine the design to more accurately produce an ideal working device.

Currently, all fabrication efforts for a prototype were not feasible if this were to become a commercial product. In the case that this device does become a commercial product,

maxon

47

the fabrication of each part would be sourced out thus creating cheaper and more available products and materials.

7.2 Potential Improvements

Possible improvements to the design of the device would result in a smoother, less intrusive experience for the user. One instance can be seen in the weight of the overall device. To minimize the weight of the device, the team believes the extensions should be manufactured out of a lightweight polymer that still allows the device to provide enough strength and flexibility to aid the user. Additionally, the standardized carbon steel gears used for the design are rather heavy and add unnecessary weight. These can also be made out of a lightweight polymer to minimize the weight of the device. From the robotics and biomedical perspective, it would be beneficial to purchase motors that are lighter in weight, and apply one to either side of the knee. This would make for a more uniform motion, and reduce the amount of stress on a single side of the device. These changes would result in added mobility for the end-user, and with a lower overall weight - reduce the required torque of the motor.

Other changes that would improve the design include adding compliance to provide another factor of safety for the user. The device already has an elastic component for the material that wraps around the users leg allowing some compliance between the user and the hinge and extensions. Additionally, incorporating a circular spring mechanism between the hinges would slow the device down as it reaches mechanical stops - storing energy at the minimum angle of flexion. Another change would be the addition of a remote button that could allow for a manual, teleoperated mode if the autonomous mode were to malfunction.

7.3 Novelty

This device intends to offer features that are unique in the current marketplace for assistive knee devices. As mentioned in the background, other devices offer various designs including a slim brace which secures the whole leg (upper quad to foot), or a larger

maxon

exoskeleton that assists both legs. These devices can be actuated by either hydraulics or motors and work in tandem with sensors that allow controlled movement of the brace. However, these factors increase the cost of the device to a premium. The team intended for the their knee brace to be a cheaper alternative for those who need less assistance. Some target markets include physical therapy patients, older populations with weak knees, and more generally for those with irregular stair gait patterns. The current design uses a combination of an EMG with a motor to drive the device. This is an intuitive control system which when refined, could increase the ease of use for users. A planetary gear system is used to increase the torque of the device while keeping the design relatively compact.

From a marketability perspective, by comparison to other existing devices, this device would need to be sold for roughly $10,000. At this price point the team believes that enough profit would be recovered after the costs of parts and labor. With added investment, such as Venture Capitalists, the cost could be as high as $15,000 while maintaining most of the target market.

Due to the novelty of the active assistive device, the team intends to seek a patent. The team believes it has marketable potential to fill a void for groups as mentioned above. The project was an excellent engineering design exercise where the team, comprised of different majors and skillsets, aimed to solve a common real-life issue.

References

Abbas, S., & Abdulhassan, Z. (2013). Kinematic Analysis of Human Climbing up and Down Stairs at Different Inclinations. *Journal of Engineering and Technology*, *31*(8), 1556–1566.

Abustan, M. S., Ali, M. F., & Talib, S. H. (2018). A case study of energy expenditure based on walking speed reduction during walking upstairs situation at a staircase in FKAAS, UTHM, Johor building. *IOP Conference Series: Earth and Environmental Science*, *140*(1). doi: 10.1088/1755-1315/140/1/012080

Adafruit. (2016). *Getting Started with MyoWare Muscle Sensor.* Retrieved from `https://learn.adafruit.com/getting-started-with-myoware-muscle-sensor`

Adiputra, L. S., Parasuraman, S., Khan, M. K., & Elamvazuthi, I. (2015). *Bio mechanics of Desending and Ascending Walk* (Vol. 76). doi: 10.1016/j.procs.2015.12.285

Alex Hernandez. (2018). *The Ottobock C-Brace is giving mobility back to some users who've lost it.* Retrieved from `https://techaeris.com/2018/09/28/the-ottobock-c-brace-is-giving-mobility-back-to-some-users-whove-lost-it/`

Automated EMG Analysis. (n.d.). Retrieved from `https://www.biopac.com/application/emg-electromyography/advanced-feature/automated-emg-analysis/`

Biron Health Group. (n.d.). *What is a musculoskeletal disorder (MSD)?* Retrieved from `https://www.biron.com/en/education-center/neat-little-guide/musculoskeletal-disorders/`

Campbell, H., & Chittenden, K. (n.d.). *What causes muscular imbalances? — Evaluating & Measuring Fitness - Sharecare.* Retrieved from `https://www.sharecare.com/health/evaluating-measuring-fitness-levels/what-causes-muscular-imbalances`

Cyberdyne. (n.d.). *HAL Single Joint - Exoskeleton Report.* Retrieved from `https://exoskeletonreport.com/product/hal-single-joint/`

maxon

Cyberdyne. (2020). *HAL FOR WELL-BEING (SINGLE JOINT TYPE).* Retrieved from `https://www.cyberdyne.jp/english/products/SingleJoint.html`

Electromyography (EMG). (2019). *Mayo Clinic*. Retrieved from `https://www.mayoclinic.org/tests-procedures/emg/about/pac-20393913`

Elina33. (2014). Vector - Anatomy of the knee joint side view, template for training a medical surgical poster, traumatology page. *123RF*. Retrieved from `https://www.123rf.com/clipart-vector/ligament.html?sti=nezhyk6hi65p4vxnbb%7C`

Frisch, D. N., & McClure, G. (n.d.). *Range of Motion (ROM) After Knee Replacement Surgery: The Basics.* Retrieved from `https://www.peerwell.co/blog/2017/07/05/range-of-motion-after-knee-replacement/`

Holicky, R. (2016). *Ottobock C-Brace: Normalizing the Gait Cycle.* Retrieved from `https://www.newmobility.com/2016/05/ottobock-c-brace/`

Kaim, C. S. (2000). *The World of Planetary Gears — Machine Design.* Retrieved from `https://www.machinedesign.com/mechanical-motion-systems/article/21834331/the-world-of-planetary-gears`

Karadsheh, M. (2020). *Knee Biomchanics.* Retrieved from `https://www.orthobullets.com/recon/9065/knee-biomechanics`

Kazamel, M., & Warren, P. (2017). History of electromyography and nerve conduction studies: A tribute to the founding fathers. *PubMed*. Retrieved from `https://www.ncbi.nlm.nih.gov/pubmed/28629678` doi: 10.1016/j.jocn.2017.05.018

Keeogo. (n.d.). *The Science Behind the Walking Aid Exoskeleton Technology — Keeogo^{TM}.* Retrieved from `https://keeogo.com/about-keeogo/the-science`

Keeogo. (2015). *Keeogo - Soldier Systems Daily.* Retrieved from `https://soldiersystems.net/tag/keeogo/`

Kohara Gear Industry. (2015). *Gear Systems — KHK Gears.* Retrieved from `https://khkgears.net/new/gear_knowledge/gear_technical_reference/gear_systems.html`

Komistek, R. D., Dennis, D. A., & Mahfouz, M. (2003, 5). In vivo fluoroscopic analysis of the normal human knee. In *Clinical orthopaedics and related research* (pp. 69–81).

Lippincott Williams and Wilkins. doi: 10.1097/01.blo.0000062384.79828.3b

Kutzner, I., Heinlein, B., Graichen, F., Bender, A., Rohlmann, A., Halder, A., . . .
Bergmann, G. (2010, 8). Loading of the knee joint during activities of daily living
measured in vivo in five subjects. *Journal of Biomechanics*, *43*(11), 2164–2173. doi:
10.1016/j.jbiomech.2010.03.046

Lafortune, M. A., Cavanagh, P. R., Sommer, H. J., & Kalenak, A. (1992). Three-
dimensional kinematics of the human knee during walking. *Journal of Biomechanics*,
25(4), 347–357. doi: 10.1016/0021-9290(92)90254-X

Ltd., S. T. C. (2020). *Grove-EMG detector.* Retrieved from `https://wiki.seeedstudio`
`.com/Grove-EMG_Detector/`

Mauney, M., Connolly, K., Dr. Aimee V. Hachigian-Gould, Mulcahy, H., & Chew, F. S.
(2013, 12). *Knee Replacement: Features and imaging assessment* (Vol. 201) (No. 6).
Retrieved from `https://www.drugwatch.com/knee-replacement/` doi: 10.2214/
AJR.13.11307

maxon - Online Shop — maxon group. (n.d.). Retrieved from `https://www.maxongroup`
`.com/maxon/view/product/control/Positionierung/520886`

Mcgibbon, C. A., Sexton, A., Jayaraman, A., Deems-Dluhy, S., Gryfe, P., Novak, A., . . .
Bonato, P. (2018). Evaluation of the Keeogo exoskeleton for assisting ambulatory
activities in people with multiple sclerosis: an open-label, randomized, cross-over
trial. *Journal of NeuroEngineering and Rehabilitation*, *15*. Retrieved from `https://`
`doi.org/10.1186/s12984-018-0468-6` doi: 10.1186/s12984-018-0468-6

Momcilovic, M. M. (2010). *Joint Moments and Powers in Healthy Young
Adults During Stair Negotiation* (Doctoral dissertation, University of Ne-
braska). Retrieved from `https://digitalcommons.unomaha.edu/cgi/`
`viewcontent.cgi?referer=https://www.google.com/&httpsredir=1&article=`
`1005&context=studentwork`

Morrison, J. B. (1970). The mechanics of the knee joint in relation to normal walking.
Journal of Biomechanics, *3*(1), 51–61. doi: 10.1016/0021-9290(70)90050-3

MyoWare. (2015). *3-lead Muscle / Electromyography Sensor for Microcontroller*

Applications. Retrieved from `https://cdn.sparkfun.com/datasheets/Sensors/Biometric/MyowareUserManualAT-04-001.pdf`

Neumann, S., Mass, S., Waldmann, D., Ricci, P.-L., Zürbes, A., Arnoux, P.-J., & Kelm, J. (2015). Design, Repeatability, and Comparison to Literature Data of a New Noninvasive Device Called "Rotameter" to Measure Rotational Knee Laxity. *International Scholarly Research Notices*, *2015*. doi: 10.1155/2015/439095

NHS. (2019, 8). *Knee replacement - NHS.* Retrieved from `https://www.nhs.uk/conditions/knee-replacement/`

Novak, A. C., Reid, S. M., Costigan, P. A., & Brouwer, B. (2010). *Stair negotiation alters stability in older adults — Lower Extremity Review Magazine.* Retrieved from `https://lermagazine.com/article/stair-negotiation-alters-stability-in-older-adults`

Olney, S. J., & Eng, J. (n.d.). *Gait — Joint Structure and Function: A Comprehensive Analysis, 5e — F.A. Davis PT Collection — McGraw-Hill Medical* (Fifth ed.). McGraw-Hill. Retrieved from `https://fadavispt.mhmedical.com/content.aspx?bookid=1862&sectionid=136086727#136086874`

Orenstein, B. W., & Sinha, S. (2018, 11). *8 Assistive Devices for Knee Osteoarthritis.* Retrieved from `https://www.everydayhealth.com/hs/osteoarthritis/knee-osteoarthritis-assistive-devices/`

OSDN. (2020). *TeraTerm.* Retrieved from `https://ttssh2.osdn.jp/index.html.en`

Ottobock. (2018). *Step into your future . The new C-Brace.*

Physiopedia. (2020). *Gait.* Retrieved from `https://www.physio-pedia.com/Gait`

Raez, M., Hussain, M., & Mohd-Yasin, F. (2006). Techniques of EMG signal analysis: detection, processing, classification and applications. *NCBI*. Retrieved from `https://www.ncbi.nlm.nih.gov/pmc/articles/PMC1455479/` doi: 10.1251/bpo115

Redfern, M. S., Cham, R., Gielo-Perczak, K., Grönqvist, R., Hirvonen, M., Lanshammar, H., ... Powers, C. (2010). Biomechanics of slips. *Ergonomics*, *44*(13).

Ren, L., Jones, R. K., & Howard, D. (2007). Predictive modelling of human walking over a complete gait cycle. *Journal of Biomechanics*, *40*(7), 1567–1574. doi: 10.1016/

j.jbiomech.2006.07.017

Screw-home mechanism. (2012). *OrthopaedicsOne The Orthopaedic Knowledge Network*.

Singh, S. (2019, 5). *Orthopedic Braces & Supports Market Worth $5.5 Billion by 2024 - Exclusive Report by MarketsandMarkets^{TM}* (Tech. Rep.). Retrieved from `https://www.prnewswire.com/news-releases/orthopedic-braces--supports-market-worth-5-5-billion-by-2024--exclusive-report-by-marketsandmarkets-300854944.html`

SuitX. (n.d.). *LegX — suitX.* Retrieved from `https://www.suitx.com/legx`

Susi, M. (2015). *UNIVERSITY OF CALGARY Gait Analysis for Pedestrian Navigation Using MEMS Handheld Devices.* Retrieved from `https://www.researchgate.net/publication/265143449_UNIVERSITY_OF_CALGARY_Gait_Analysis_for_Pedestrian_Navigation_Using_MEMS_Handheld_Devices`

Technologies, A. (n.d.). *DIY Muscle Sensor / EMG Circuit for a Microcontroller.* Retrieved from `https://www.instructables.com/id/Muscle-EMG-Sensor-for-a-Microcontroller/`

Van der Plas, A., & Bloem, J. (2016). *X-knee - Startradiology.* Retrieved from `https://www.startradiology.com/internships/orthopedics/knee/x-knee/`

Vicon. (2020). *Full Body Modeling with Plug-in Gait.* Retrieved from `https://docs.vicon.com/display/Nexus26/Full+body+modeling+with+Plug-in+Gait`

Webb, A. G. (2018). Surface Electrode Design. In *Principles of biomedical instrumentation* (pp. 27–30). Cambridge University Press. doi: 10.1017/9781316286210

What is a Voltage Follower. (2020). Retrieved from `http://www.learningaboutelectronics.com/Articles/Voltage-follower`

Appendix A   Existing Device Comparison

Device	Weight	Price	Purpose
Ottobock C-Brace ®	*Unknown*	*~$75,000*	*High level of active assistance*
LegX ®	*6.2 kg*	*$5,000+*	*Industrial work/heavy lifting*
MIT Rheo ® Knee	*1.61 kg*	*$35,000+*	*For amputees, full replacement of knee*
Keeogo ®	*5.4 kg*	*$30,000+*	*High level of active assistance*
HAL ® (single joint)	*1.5 kg*	*Unknown*	*Medium/Low level of active assistance over low duration*

maxon

Appendix B   Maxon Group Motor Catalog Page

EC 90 flat ∅90 mm, brushless, 220 Watt
Open Rotor

maxon flat motor

V1

0
24.9 -0.4   27.4 max.

0
5.4 -0.2   6.5

⌀ 0.05 A

A

0.2 max.

∅90 ±0.1

59

0   -0.05
∅35 -0.007
∅10 -0.014

PIN 1
PIN 5

40

12.8

V2

M5x5.8
tief/deep   ⌖ ∅0.2 A

34±20°

∅ 65

R5.6

300 ±10

30

PIN 4 — PIN 6
PIN 1 — PIN 3

PIN 3 — PIN 4
PIN 1 — PIN 2

M 1:4

Stock program
Standard program
Special program (on request)

Part Numbers

V1 with Hall sensors	607942	607943	607944
V2 with Hall sensors and cables	607946	607947	607948

Motor Data

Values at nominal voltage					
1 Nominal voltage	V	24	36	60	
2 No load speed	rpm	3170	3070	2600	
3 No load current	mA	658	420	197	
4 Nominal speed	rpm	2490	2420	2020	
5 Nominal torque (max. continuous torque)	mNm	729	715	692	
6 Nominal current (max. continuous current)	A	9.44	6.01	2.96	
7 Stall torque[1]	mNm	7910	7580	6410	
8 Stall current	A	111	68.9	29.6	
9 Max. efficiency	%	85.4	85.2	84.6	
Characteristics					
10 Terminal resistance phase to phase	Ω	0.216	0.523	2.03	
11 Terminal inductance phase to phase	mH	0.232	0.554	2.15	
12 Torque constant	mNm/A	71.2	110	217	
13 Speed constant	rpm/V	134	86.8	44.1	
14 Speed/torque gradient	rpm/mNm	0.407	0.412	0.412	
15 Mechanical time constant	ms	13.5	13.7	13.7	
16 Rotor inertia	gcm²	2875	2875	2875	

Specifications

Thermal data
17 Thermal resistance housing-ambient   1.87 K/W
18 Thermal resistance winding-housing   1.43 K/W
19 Thermal time constant winding   27.7 s
20 Thermal time constant motor   278 s
21 Ambient temperature   -40...+100°C
22 Max. winding temperature   +125°C

Mechanical data (preloaded ball bearings)
23 Max. speed   5000 rpm
24 Axial play at axial load   0.14 mm
25 Radial play   preloaded
26 Max. axial load (dynamic)   34 N
27 Max. force for press fits (static)   440 N
(static, shaft supported)
28 Max. radial load, 10 mm from flange   100 N

Other specifications
29 Number of pole pairs   11
30 Number of phases   3
31 Weight of motor   624 g
Values listed in the table are nominal.

Connection V1	V2 (sensors, AWG 24)
Pin 1 Hall sensor 1	Hall sensor 1
Pin 2 Hall sensor 2	Hall sensor 2
Pin 3 V_{Hall} 4.5...24 VDC	Hall sensor 3
Pin 4 Motor winding 3	GND
Pin 5 Hall sensor 3	V_{Hall} 4.5...24 VDC
Pin 6 GND	N.C.
Pin 7 Motor winding 1	
Pin 8 Motor winding 2	

V2 (motor, AWG 16)
Pin 1   Motor winding 1
Pin 2   Motor winding 2
Pin 3   Motor winding 3
Pin 4   N.C.
Wiring diagram for Hall sensors see p. 47

Connector	Part number
Molex 46015-0806	43025-0600
Molex 39-01-2040	

Connection cable for V1
Connection cable Universal, L = 500 mm   **339380**
Connection cable to EPOS4, L = 500 mm   **354045**
[1]Calculation does not include saturation effect
(p. 57/162)

Operating Range   Comments

n [rpm]
6000
5000
4000
3000
2000
1000
0

220 W

607942

0   500   1000   M [mNm]
0.64   7   13   I [A]

Continuous operation
In observation of above listed thermal resistance (lines 17 and 18) the maximum permissible winding temperature will be reached during continuous operation at 25°C ambient.
= Thermal limit.

Short term operation
The motor may be briefly overloaded (recurring).

Assigned power rating

maxon Modular System   Details on catalog page 36

Encoder MILE
512 - 6400 CPT,
2 channels
Page 414

Recommended Electronics:
Notes   Page **36**
ESCON Mod. 50/5   455
ESCON Mod. 50/8 (HE)   456
ESCON 50/5   457
ESCON 70/10   457
DEC Module 50/5   459
EPOS4 50/5   463
EPOS4 Mod./Comp. 50/5   463
EPOS4 Mod./Comp. 50/8   465
EPOS4 Mod./Comp. 50/15   466
EPOS4 70/15   467
MAXPOS 50/5   473

maxon EC motor 271

Appendix C   MyoWare Code

```
const int analogInPin = A0;  // Analog input pin that the potentiometer is attached to
const int analogOutPin = 9; // Analog output pin that the LED is attached to

int sensorValue = 0;         // value read from the pot
int outputValue = 0;         // value output to the PWM (analog out)

void setup() {
  // initialize serial communications at 9600 bps:
  Serial.begin(9600);
}

void loop() {
  // read the analog in value:
  sensorValue = analogRead(analogInPin);
  // map it to the range of the analog out:
  outputValue = map(sensorValue, 0, 1023, 0, 255);
  // change the analog out value:
  analogWrite(analogOutPin, outputValue);

  // print the results to the Serial Monitor:
  Serial.print(millis());
  Serial.print(",");
  Serial.print("\t");
  Serial.print(outputValue);
  Serial.println();


  // wait 2 milliseconds before the next loop for the analog-to-digital
  // converter to settle after the last reading:
  delay(2);
}
```

Appendix D   EMG Code

```
// Grove - EMG Sensor demo code
// This demo will need a Grove - Led Bar to show the motion
// Grove - EMG Sensor connect to A0
// Grove - LED Bar connect to D8, D9
// note: it'll take about serval seconds to detect static analog value
// when you should hold your muscle static. You will see led bar from level 10 turn to
// level 0, it means static analog value get ok

#include <Grove_LED_Bar.h>

Grove_LED_Bar bar(9, 8, 0);

int max_analog_dta      = 300;              // max analog data
int min_analog_dta      = 100;              // min analog data
int static_analog_dta   = 0;                // static analog data
int getAnalog(int pin)                      // get analog value
{    long sum = 0;

     for(int i=0; i<32; i++) {
         sum += analogRead(pin);}
     int dta = sum>>5;
     max_analog_dta = dta>max_analog_dta ? dta : max_analog_dta;      // if max data
     min_analog_dta = min_analog_dta>dta ? dta : min_analog_dta;      // if min data
     return sum>>5;}

void setup() {
    Serial.begin(115200);
    long sum = 0;
    for(int i=0; i<=10; i++) {
        for(int j=0; j<100; j++) {
            sum += getAnalog(A0);
            delay(1);}
        bar.setLevel(10-i);}
    sum /= 1100;
    static_analog_dta = sum;
    Serial.print("static_analog_dta = ");
    Serial.println(static_analog_dta);}
int level       = 5;
int level_buf   = 5;

void loop() {
    int val = getAnalog(A0);                    // get Analog value
    int level2;
    if(val>static_analog_dta)                   // larger than static_analog_dta
    {level2 = 5 + map(val, static_analog_dta, max_analog_dta, 0, 5);}
    else
    {level2 = 5 - map(val, min_analog_dta, static_analog_dta, 0, 5);}
    // to smooth the change of led bar
    if(level2 > level)
    {level++;}
    else if(level2 < level)
    {level--; }
    if(level != level_buf)
    {level_buf = level;
     bar.setLevel(level);}
    Serial.println(getAnalog(A0));
    delay(10);
}
```

maxon   58

Appendix E   SolidWorks Simulation

Appendix F   3D Model SolidWorks Drawings

Drawing annotations:

- 3X Ø 5.35 ▽ 10.00
- ∨ Ø 10.40 X 90°
- Ø 4.20 THRU
- 19.31
- 23.03°
- 22.02
- 20.96
- 58.95°
- 90°
- R 4.00
- R8.01
- Ø 35.01
- 5.00
- 47.35
- Ø 110.03
- 72.00
- 21.11
- Ø 8.00
- Ø 4.20 THRU
- Ø 4.20 THRU
- 3X Ø 5.35 ▽ 10.00
- ∨ Ø 10.40 X 90°
- Ø 16.01 THRU
- Ø 5.41 ▽ 5.23
- Ø 5.41 ▽ 5.23
- Ø 100.03
- Ø 110.03
- 5.00
- 28.02
- Ø 110.03

Title block:

UNLESS OTHERWISE SPECIFIED:

DIMENSIONS ARE IN INCHES
TOLERANCES:
FRACTIONAL ±
ANGULAR: MACH ±   BEND ±
TWO PLACE DECIMAL ±
THREE PLACE DECIMAL ±

INTERPRET GEOMETRIC TOLERANCING PER:

MATERIAL
6061 Aluminum

FINISH

DO NOT SCALE DRAWING

	NAME	DATE
DRAWN	Christina Steele	
CHECKED		
ENG APPR.		
MFG APPR.		
Q.A.		
COMMENTS:		

TITLE:
Active Assistive Knee Device: Female Hinge

SIZE **B**   DWG. NO. V6 Female Hinge   REV

SCALE: 1:1   WEIGHT: SHEET 1 OF 1

NEXT ASSY   USED ON
APPLICATION

R15.50 THRU
R24.50 THRU
Ø 100.00
R38.00 � 6.80
Ø 13.00 THRU

8.72
21.19
Ø 2.15
19.50
97.70
Ø 100.00
25.70
R4.00
2X Ø 4.20 � 9.50
⍌ Ø 10.40 X 90°
30.02
13.50
6.00

1.02
R4.00
Ø 13.000 THRU
Ø 100.00
Ø 89.92 � 10.00
2X Ø 4.20 � 9.50
⍌ Ø 10.40 X 90°

UNLESS OTHERWISE SPECIFIED:
DIMENSIONS ARE IN INCHES
TOLERANCES:
FRACTIONAL±
ANGULAR: MACH±   BEND ±
TWO PLACE DECIMAL ±
THREE PLACE DECIMAL ±

INTERPRET GEOMETRIC
TOLERANCING PER:
MATERIAL
6061 Aluminum
FINISH

DO NOT SCALE DRAWING

NAME   DATE
DRAWN   Christina Steele
CHECKED
ENG APPR.
MFG APPR.
Q.A.
COMMENTS:

PROPRIETARY AND CONFIDENTIAL
THE INFORMATION CONTAINED IN THIS
DRAWING IS THE SOLE PROPERTY OF
<INSERT COMPANY NAME HERE>. ANY
REPRODUCTION IN PART OR AS A WHOLE
WITHOUT THE WRITTEN PERMISSION OF
<INSERT COMPANY NAME HERE> IS
PROHIBITED.

NEXT ASSY   USED ON
APPLICATION

TITLE:
Active Assistive Knee
Device Male Hinge

SIZE   DWG. NO.   REV
B   V6 Male Hinge

SCALE: 1:1   WEIGHT: SHEET 1 OF 1

Appendix G   Product Specification Sheet

Product Specification Sheet
Active Assistive Knee Device
Team: Zachary Zlotnick, Christina Steele, Kassidy Utheim,
Jason McGrath, Tina Barsoumian

Product Description:

The active assistive knee device (patent pending) features a powerful 220W brushless motor to provide the necessary torque for users of most shapes and sizes. The ergonomic design allows customization at the upper and lower leg contact points, and can be adjusted to provide varying levels of assistance. Sensing your gait while ascending or descending stairs, this nonintrusive device will provide an assistive torque in the required direction. Both configurable and intuitive, the assistive knee device allows the user a helping hand for their daily mobility-related needs.

Product Features and Specifications:

◊ Planetary gear drive - Translates speed into torque, to allow maximum torque output in a compact design at a 3:1 ratio

◊ Adjustable - Zip-up sleeve has (insert number) different fits for legs of all sizes

◊ Configurable - Adjustable torque based on consumer needs

◊ Open Rotor Brushless Motor - Flat design reduces thickness and attaches easily to hinge joint

◊ EMG - Senses your movement in order to provide ample assistance at the right time

◊ Lightweight exoskeleton – the user maintains freedom of movement

Product Name	Assistive Torque Device	**Microcontroller**	Arduino Uno
Cost	$10,000	**Recommended Height**	5'2"-6'2"
Color	Silver, Grey, Black	**Recommended Weight**	60-90kg
Dimensions	200x110x60 (mm)	**Materials**	1065 Aluminum, Carbon Steel
Weight	4.5lb.	**Additional Info**	Patent Pending

maxon